Acoustic classification of Atlantic capelin (*Mallotus villosus*) and its abundance in the Gulf of St. Lawrence between 2016 and 2020

Shani Rousseau

Regional Sciences Branch
Quebec Region
Pelagic and Ecosystemic Sciences Division
Fisheries and Oceans Canada
Maurice Lamontagne Institute
850, Route de la Mer
Mont-Joli, QC
G5H 3Z4

2026

Canadian Technical Report of
Fisheries and Aquatic Sciences 3812

Fisheries and Oceans Canada | Pêches et Océans Canada

Canada

Canadian Technical Report of Fisheries and Aquatic Sciences

Technical reports contain scientific and technical information that contributes to existing knowledge but which is not normally appropriate for primary literature. Technical reports are directed primarily toward a worldwide audience and have an international distribution. No restriction is placed on subject matter and the series reflects the broad interests and policies of Fisheries and Oceans Canada, namely, fisheries and aquatic sciences.

Technical reports may be cited as full publications. The correct citation appears above the abstract of each report. Each report is abstracted in the data base *Aquatic Sciences and Fisheries Abstracts*.

Technical reports are produced regionally but are numbered nationally. Requests for individual reports will be filled by the issuing establishment listed on the front cover and title page.

Numbers 1-456 in this series were issued as Technical Reports of the Fisheries Research Board of Canada. Numbers 457-714 were issued as Department of the Environment, Fisheries and Marine Service, Research and Development Directorate Technical Reports. Numbers 715-924 were issued as Department of Fisheries and Environment, Fisheries and Marine Service Technical Reports. The current series name was changed with report number 925.

Rapport technique canadien des sciences halieutiques et aquatiques

Les rapports techniques contiennent des renseignements scientifiques et techniques qui constituent une contribution aux connaissances actuelles, mais qui ne sont pas normalement appropriés pour la publication dans un journal scientifique. Les rapports techniques sont destinés essentiellement à un public international et ils sont distribués à cet échelon. II n'y a aucune restriction quant au sujet; de fait, la série reflète la vaste gamme des intérêts et des politiques de Pêches et Océans Canada, c'est-à-dire les sciences halieutiques et aquatiques.

Les rapports techniques peuvent être cités comme des publications à part entière. Le titre exact figure au-dessus du résumé de chaque rapport. Les rapports techniques sont résumés dans la base de données *Résumés des sciences aquatiques et halieutiques.*

Les rapports techniques sont produits à l'échelon régional, mais numérotés à l'échelon national. Les demandes de rapports seront satisfaites par l'établissement auteur dont le nom figure sur la couverture et la page du titre.

Les numéros 1 à 456 de cette série ont été publiés à titre de Rapports techniques de l'Office des recherches sur les pêcheries du Canada. Les numéros 457 à 714 sont parus à titre de Rapports techniques de la Direction générale de la recherche et du développement, Service des pêches et de la mer, ministère de l'Environnement. Les numéros 715 à 924 ont été publiés à titre de Rapports techniques du Service des pêches et de la mer, ministère des Pêches et de l'Environnement. Le nom actuel de la série a été établi lors de la parution du numéro 925.

Canadian Technical Report of
Fisheries and Aquatic Sciences 3812

2026

Acoustic classification of Atlantic capelin (*Mallotus villosus*) and its abundance in the Gulf of St. Lawrence between 2016 and 2020

Shani Rousseau

Regional Sciences Branch
Quebec Region
Pelagic and Ecosystemic Sciences Division
Fisheries and Oceans Canada
Maurice Lamontagne Institute
850, Route de la Mer
Mont-Joli, QC
G5H 3Z4

© His Majesty the King in Right of Canada, as represented by the Minister of the Department of Fisheries and Oceans, 2026

This work is licensed under the Open Government Licence

Cat. No. Fs 97-6/3812E-PDF ISBN 978-1-100-00802-8 ISSN 1488-5379

https://doi.org/10.60825/q7gp-xv74

Correct citation for this publication:

Rousseau, S. 2026. Acoustic classification of Atlantic capelin (*Mallotus villosus*) and its abundance in the Gulf of St. Lawrence between 2016 and 2020. Can. Tech. Rep. Fish. Aquat. Sci. 3812: vii + 29 p. https://doi.org/10.60825/q7gp-xv74

TABLE OF CONTENTS

LIST OF FIGURES iv
LIST OF TABLES v
ABSTRACT vi
RÉSUMÉ vii
1. Introduction 1
2. Methods 2
2.1 Data acquisition 2
2.2 Data processing and analysis 3
2.3 Acoustic scattering within the cold intermediate layer 5
2.4 Machine learning classification models 5
2.5 Bottom trawl species composition 7
2.6 Exclusion of strata 7
2.7 Biomass estimation 8
3. Results 8
3.1 ML model performance 8
3.2 Capelin abundance 9
3.3 Capelin distribution 9
4. Discussion 10
4.1 ML classification 10
4.2 Catchability 11
4.3 Capelin abundance 12
5. Conclusion 13
Acknowledgements 15
References 16
Tables 20
Figures 21

LIST OF FIGURES

Figure 1. NAFO Divisions in the Gulf of St. Lawrence and the Newfoundland regions, and stratum definitions for the nGSL and sGSL annual bottom trawl surveys (grey polygons). Note that Divisions 3P and 2J are not included in this study. 21
Figure 2. Standardized mean trawl biomass by stratum between 2016 and 2020 in the nGSL as obtained from the bottom trawl surveys. Shaded areas show strata excluded from method "STRAT". Red line represents the 5 kg cut off for exclusion of the stratum based on Atlantic herring and/or cod biomass. 22
Figure 3. Standardized mean trawl biomass by stratum between 2016 and 2020 in the sGSL as obtained from the bottom trawl surveys. Shaded areas show strata excluded from method "STRAT". Red line represents the 5 kg cut off for exclusion of the stratum based on Atlantic herring and/or cod biomass. 22
Figure 4. F1 score and Accuracy K as a function of the number of variables including (left panels) and excluding (right panels) the depth variables for the SVM with a radial kernel. 23
Figure 5. Total annual capelin biomass in the nGSL obtained with the classification methods presented in this study, as well as biomass derived from the bottom trawl survey ("CATCH"). ..23
Figure 6. Total annual capelin biomass in the sGSL obtained with the classification methods presented in this study, as well as biomass derived from the bottom trawl survey ("CATCH"). ..24
Figure 7. Total annual capelin biomass in the GSL obtained with the classification methods presented in this study, as well as biomass derived from the bottom trawl survey ("CATCH") from 1990 to 2020. 24
Figure 8. Mean biomass density (kg m^{-2}) estimated with method "CIL", all years of the acoustic study combined (2016-2020). 25
Figure 9. Mean biomass density (kg m^{-2}) estimated with method "STRAT", all years of the acoustic study combined (2016-2020). Excluded strata as shown in Figures 2 and 3 are shaded. 25
Figure 10. Mean biomass density (kg m^{-2}) estimated with method "COMP", all years of the acoustic study combined (2016-2020). 26
Figure 11. Mean biomass density (kg m^{-2}) estimated with the SVM, all years of the acoustic study combined (2016-2020). 26
Figure 12. Mean biomass density (kg m^{-2}) from bottom trawl catch data ("CATCH"), all years of the acoustic study combined (2016-2020). 27
Figure 13. Mean volume backscattering coefficient (sv m^{-1}) corresponding to swim bladdered fish within the CIL boundaries for each year of the acoustic study, using methods "CIL" and "STRAT", as a function of the distance separating the CIL from the seafloor, in the GSL. 27
Figure 14. Mean area scattering coefficient (sa, m^2 m^{-2}) corresponding to swim bladdered fish within the CIL boundaries for each year of the acoustic study, using methods "CIL" and "STRAT", as a function of the distance separating the CIL from the seafloor, in the GSL. sa is equal to sv multiplied by the CIL thickness. 28
Figure 15. Bottom depth density functions corresponding to the 2446 observations used in the ML models. 28
Figure 16. Total biomass in the nGSL and the sGSL including and excluding night time sampling, estimated with methods "CIL" and "STRAT". 29

LIST OF TABLES

Table 1. Summary of the surveys used to train the capelin classification models. All surveys were conducted onboard the CCGS Teleost. 20
Table 2. Summary of samples used in the classification model before balancing the dataset. Each observation represents a 100 ping by 5 meter averaged sample. 20
Table 3. TS to length relationships used in the calculation of capelin biomass and to separate acoustic scattering following species composition in the trawl (method “COMP”). 20
Table 4. Model best performance on the validation data set, with corresponding variables, using the initial hyperparameters described in section 2.4. In the model names, *r* stands for radial, *l* for linear, and *a* refers to models that only used acoustic variables. 20

ABSTRACT

Rousseau, S. 2026. Acoustic classification of Atlantic capelin (*Mallotus villosus*) and its abundance in the Gulf of St. Lawrence between 2016 and 2020. Can. Tech. Rep. Fish. Aquat. Sci. 3812: vii + 29 p. https://doi.org/10.60825/q7gp-xv74

This study evaluates the feasibility of developing an acoustic abundance index for Atlantic capelin in the Gulf of St. Lawrence using opportunistically collected acoustic data from multispecies bottom-trawl surveys. Several classification approaches were developed, including machine learning models and methods based on acoustic characteristics, trawl data, and environmental criteria. Excluding depth variables, the radial support vector machine showed the highest performance among the machine learning models examined (F1 score = 0.74; Accuracy K = 0.74).

Acoustic methods produced similar interannual patterns in capelin abundance across the time series, with the exception of 2017. Estimated total biomass varied among methods, ranging from 1 976 t to 32 716 t, and were low compared to commercial catch data. Catchability estimates were derived from comparisons between acoustic and bottom-trawl survey data, yielding values of 0.58 ± 0.32 when the CIL intersected with the seafloor, and 0.22 ± 0.12 when it was located higher in the water column. Spatial patterns showed localized areas of higher abundance, particularly along the shore in the northern Gulf and estuary, south of the Gaspé peninsula, in the Strait of Belle Isle and south of Anticosti Island. Differences in biomass estimates were observed between day and night in some regions and years.

Despite uncertainties, this study demonstrates that opportunistically collected acoustic data, combined with appropriate classification methods, can provide a useful complementary index of Atlantic capelin abundance and distribution in the Gulf of St. Lawrence.

RÉSUMÉ

Rousseau, S. 2026. Acoustic classification of Atlantic capelin (*Mallotus villosus*) and its abundance in the Gulf of St. Lawrence between 2016 and 2020. Can. Tech. Rep. Fish. Aquat. Sci. 3812: vii + 29 p. https://doi.org/10.60825/q7gp-xv74

Cette étude évalue la possibilité de développer un indice d'abondance acoustique pour le capelan atlantique dans le golfe du Saint-Laurent à partir de données acoustiques récoltées de manière opportuniste lors de relevés multi-espèces au chalut de fond. Plusieurs approches de classification ont été développées, incluant des modèles d'apprentissage automatique ainsi que des méthodes basées sur les caractéristiques acoustiques, les données de chalutage et des critères environnementaux. En excluant les variables de profondeur, le modèle de machine à vecteurs de support radial a montré les meilleures performances parmi les modèles d'apprentissage automatique (score F1 = 0,74; exactitude K = 0,74).

Les méthodes basées sur l'acoustique ont produit des tendances interannuelles similaires de l'abondance du capelan atlantique au cours de la série temporelle, à l'exception de l'année 2017. La biomasse totale estimée variait selon les méthodes, allant de 1 976 t à 32 716 t, et demeurait faible comparativement aux données de captures commerciales. Des estimations de capturabilité ont été obtenues à partir de comparaisons entre les données acoustiques et celles du chalutage de fond, donnant des valeurs de 0,58 ± 0,32 lorsque la Couche Intermédiaire Froide intersectait avec le fond marin, et de 0,22 ± 0,12 lorsqu'elle était située plus haut dans la colonne d'eau. Les patrons spatiaux ont révélé des zones localisées de forte abondance, notamment le long de la côte dans le nord du Golfe et dans l'estuaire, au sud de la péninsule de Gaspé, dans le détroit de Belle Isle et au sud d'Anticosti. Des différences dans les estimations de biomasse ont été observées entre les données de jour et de nuit dans certaines régions et certaines années.

Malgré les incertitudes, cette étude démontre que les données acoustiques récoltées de manière opportuniste, combinées à des méthodes de classification adéquates, peuvent fournir un indice complémentaire de l'abondance et de la répartition du capelan atlantique dans le golfe du St-Laurent.

1. INTRODUCTION

Atlantic capelin (*Mallotus villosus*, hereafter capelin) is a small cold-water pelagic forage fish distributed throughout the Arctic and sub-Arctic regions of the Pacific and Atlantic oceans. In the Gulf of St. Lawrence (GSL), capelin supports a commercial fishery and serves as a primary prey species for numerous predators, including marine mammals, seabirds, and larger fish. As a result, it occupies a central role in the structure and functioning of the GSL ecosystem.

In eastern Canada, the commercial exploitation of capelin is managed by the Newfoundland and Quebec Regions of the Department of Fisheries and Oceans (DFO). In the GSL, defined under the Northwest Atlantic Fisheries Organization (NAFO) as Divisions 4RST (Figure 1), stock status is partly assessed through a fishery-independent abundance index derived from annual bottom trawl survey data (DFO 2024; Chamberland et al. 2022). This index was developed in the absence of a fishery-independent survey specifically targeting capelin; however, its interpretation is subject to several sources of uncertainty. For instance, capelin catchability in the bottom-trawl survey is low, and the factors influencing its variability remain poorly understood. Current interpretations assume that catchability increases when the Cold Intermediate Layer (CIL), the preferred habitat for capelin, is associated with the seafloor, thereby increasing the proportion of fish available to the trawl (Chamberland et al. 2022). The index also assumes that capelin density within the CIL is largely homogeneous. To date, however, these assumptions have not been formally evaluated.

As a small, schooling pelagic species, an acoustic abundance index is the preferred assessment approach for capelin (Simmonds and MacLennan 2005). A capelin acoustic survey has been conducted on the eastern coast of Newfoundland since 1982, and is currently the main fishery-independent input for capelin stock assessment in NAFO Divisions 2J3KL (Murphy et al. 2025). Although no dedicated capelin acoustic survey exists in the GSL, active acoustic data have been collected as part of the annual bottom-trawl survey on an opportunistic basis since 2005 (although properly calibrated from 2012). These surveys do not target capelin, but they may provide sufficient spatial and temporal coverage to allow for the development of an acoustic index for capelin in the GSL.

Hydroacoustic techniques are widely employed to assess pelagic fish stocks around the world (e.g., Gjøsæter et al. 2002; Chashchin et al. 2015; DFO 2026). These methods offer several advantages in terms of resolution, spatial coverage, and cost efficiency; however, they are constrained by their species discrimination capabilities, and traditionally rely on expert interpretation of echograms, supported by trawl sampling data. This traditional approach cannot be applied in the case of opportunistically acquired acoustic data, due to the lack of direct validation of acoustic echoes through pelagic trawling. Therefore, developing an objective and accurate classification method for identifying capelin targets is a critical first step toward establishing a reliable acoustic index from such data.

Several methods have been proposed to objectively classify marine organisms in acoustic data. These methods may use acoustic (i.e. backscattered energy), morphometric (e.g. school size and shape), bathymetric (e.g. depth) or positional (e.g. location) characteristics, often using them in combination. A review of the most recent progress in acoustic target classification can be found in Korneliussen et al. (2018). As with many other fields, machine learning (ML) approaches to classify acoustic targets have received increasing attention; Rubbens et al. (2023) and Yassir et

al. (2023) both provide an overview of the most recent ML techniques applied to fisheries acoustics and other fields of marine ecology.

Deep learning approaches have shown much promise in acoustic target classification (Cabreira et al. 2009; Brautaset et al. 2020; Marques et al. 2021). However, they require large amounts of validated data to provide accurate classifications, although Choi et al. (2021) were able to reduce the need for validated data by combining a neural network with a semi-supervised clustering algorithm. Random forest models perform well with smaller datasets and have yielded good results when data were averaged within each school. This method was applied successfully, for example, to mackerel icefish (*Champsocephalus gunnari*) (Fallon et al. 2016), silver cyprinid (*Rastrineobola argentea*) (Proud et al. 2020), Pacific salmon (*Oncorhynchus* spp.) and Pacific herring (*Clupea pallasii*) (Rousseau et al. 2022). In the past decade, the most commonly used ML methods in the field of marine ecology have been the Convolutional Neural Network (CNN), Artificial Neural Network (ANN), Random Forest (RF) and Support Vector Machine (SVM).

Developing a classification model requires large amounts of high quality acoustic data that have been classified following their different background features (e.g. bottom, surface, waves and instrument noise) and species classes (e.g. krill and different species of fish). Species classes can be validated with trawl samples by matching the acoustic data to the location of the corresponding trawl sample in the water column. This study used acoustic data validated by bottom trawl samples collected during the northern GSL (nGSL) and southern GSL (sGSL) groundfish surveys, as well as acoustic data validated by a pelagic trawl during the dedicated DFO Spring capelin acoustic survey off the east coast of Newfoundland within NAFO Division 3L and the southern part of 3K.

The first objective of this study is to develop and present a machine learning approach for the acoustic classification of capelin. The second objective is to present a suite of alternative classification methods that integrate a combination of acoustic characteristics, bottom trawl data and current knowledge of capelin ecology. The third objective is to characterize the abundance and distribution of capelin in the GSL using these newly developed methods. The fourth objective is to apply the resulting classifications to address key uncertainties associated with the currently accepted bottom-trawl index for the 4RST capelin stock in the GSL.

2. METHODS

2.1 DATA ACQUISITION

Acoustic data obtained from three annual surveys between 2016 and 2021 were used (Table 1): 1) the nGSL groundfish survey, covering NAFO Divisions 4RS (Figure 1) in August (Chamberland et al. 2025); 2) the sGSL multispecies survey, taking place in NAFO Division 4T in September (Hurlbut and Clay 1990; Savoie 2014), and 3) the capelin combined acoustic-trawl survey, covering NAFO Division 3L and the southern portion of 3K conducted in May (Mowbray 2014; Murphy et al. 2025). The latter survey was used exclusively in the development of the machine learning classification models (objective 1), to provide additional reliable capelin echoes, which were difficult to obtain from the groundfish surveys. Similarly, the 2021 4RS groundfish survey was included for model training only. For objectives 2 to 4, analyses were limited to GSL acoustic data collected from 2016 to 2020, as data processing (described in section 2.2) had only been completed for those years at the time of publication.

All surveys were conducted onboard the CCGS Teleost, a vessel equipped with a hull-mounted, split-beam SIMRAD EK60 echosounder operating at four frequencies (38, 70, 120 and 200 kHz). The transducers were calibrated each year according to the standard sphere methods outlined in Demer et al. (2015). The power output was 2000 W, 750 W, 250 W and 150 W at 38 kHz, 70 kHz, 120 kHz and 200 kHz, respectively. Transmitted pulse duration was 1.024 ms and ping rate was set to 1 second or to maximum ping (the maximum rate at which the sound pulse can travel to the seafloor and back). The acoustic data were recorded continuously during the entire surveys. For the capelin dedicated acoustic survey, conductivity, temperature and depth profiles (CTD) were collected each day and used to adjust sound speed and absorption coefficient during data collection. For the nGSL and the sGSL groundfish surveys, sound speed and absorption coefficient were estimated for each daily acoustic data file by using the closest CTD cast available.

The nGSL and sGSL bottom-trawl surveys follow a stratified-random design. For each fishing tow, each species was weighted (total catch) and a subsample was collected for individual weight and length measurements. For the capelin combined acoustic-trawl survey in 3L and southern 3K, targeted pelagic trawling was conducted to validate the acoustic data for species composition. The main species of swim bladdered fish found in the GSL in the pelagic zone are capelin, Atlantic herring (*Clupea harengus*), Atlantic cod (*Gadus morhua*) and redfish (*Sebastes* spp.).

2.2 DATA PROCESSING AND ANALYSIS

The acoustic data were visualized and processed as the volume backscattering strength (S_v, dB re 1 m^{-1}), which represents the mean backscattering intensity per cubic meter, in the logarithmic domain:

$$S_v = 10log_{10}(s_v), \quad (1)$$

where

$$s_v = \frac{\sum \sigma_{bs}}{V}. \quad (2)$$

The term s_v represents the volume backscattering coefficient (m^{-1}), σ_{bs} the backscattering cross-section (m^2) and V the volume sampled (m^3). All symbols and units follow the conventions proposed by MacLennan et al. (2002).

The analyses were conducted in Echoview 14 (Myriax Pty, Ltd., Hobart, Tasmania, Australia) and the R software for statistical computing (version 4.4.1, R Core Team 2024) with RStudio (version 2024.4.2.764, RStudio Team 2024). Impulse noise was removed from the S_v echograms following the method described in Ryan et al. (2015). Areas of impulse noise were replaced by the mean of the surrounding cells. Background noise was removed following the method by De Robertis and Higginbottom (2007). A minimum signal to noise ratio of 10 dB and an averaging cell of 40 pings (one ping corresponds to one individual sound burst) and 10 vertical meters were used. The maximum noise, as described by De Robertis and Higginbottom (2007), was set to -175, -165, -160 and -155 dB at 38, 70, 120 and 200 kHz, respectively, and was determined empirically.

An attenuated acoustic signal can result from the presence of air bubbles underneath the hull and the transducer. Areas of attenuation were manually removed from the analysis. Each echogram was visually scrutinized to remove unwanted signal such as instruments in water or noise that was not successfully removed by the previously described data cleaning protocol.

Data above a depth corresponding to the transducer depth plus 5 m were excluded from the analysis. A bottom line was defined using Echoview's best bottom candidate algorithm with a minimum volume backscattering strength threshold of -70 dB and a peak threshold of -50 dB. A backstep of 0.7 m was used throughout the time series. The value of the backstep was chosen as a compromise to increase speed of analysis while retaining as much signal near the seafloor as possible.

Prior to applying the classification models, the acoustic data were simplified to exclude all scattering except that corresponding to swim bladdered fish. This approach was used to account for the high diversity of echoes found in these large scale, opportunistically collected acoustic data.

A combined frequency method based on Fernandes (2009) was used to select fish aggregations and remove unwanted weak scatterers. Fish exhibit a strong and stable acoustic amplitude across frequencies, compared to many other scatterers. As a result, combining echograms across frequencies amplifies the signal of fish, while diminishing the signal of other scatterers. This method has been used successfully in several studies (e.g. Fallon et al. 2016; Korneliussen et al. 2016; Korneliussen 2018; Rousseau and Émond 2024). It is efficient at retaining echoes from both swim bladdered and non-swim bladdered fish including Atlantic herring, capelin, mackerel (*Scomber scombrus*) and sandeel (*Ammodytes* spp.). Echograms of the volume backscattering strength were averaged following $(3S_{v_{38}} + S_{v_{120}} + S_{v_{200}})/5$, where $S_{v_{38}}$, $S_{v_{120}}$ and $S_{v_{200}}$ are the volume backscattering strength (dB re 1 m^{-1}) at 38, 120 and 200 kHz, respectively. A higher weight was attributed to the 38 kHz frequency in the average, to further reduce the weight of zooplankton echoes, which are stronger at 120 and 200 kHz. The 70 kHz frequency was excluded from this calculation to allow its application to other surveys, since this frequency is less often available. The resulting virtual echograms were smoothed with a 2D gaussian convolution kernel with a standard deviation of 1.0 and a window of 3 samples and 3 pings (approximately equivalent to 0.55 m x 18.5 m). A gaussian convolution puts a higher weight on the center pixel and emphasizes edges. It is a low pass filter – as a result isolated pixels are removed. A threshold of -85 dB was applied on the resulting echogram following a 5 x 5 dilation filter (approximately equivalent to 0.92 m x 30.83 m). This latter step helps retain all features of the aggregations including edges. Finally, a bitmap was used to mask the original S_v data at all frequencies with the virtual echogram, i.e. all true values in the bitmap were replaced with the original S_v values, while all false values were excluded from the echogram (see Fernandes 2009).

A threshold of 0 dB was applied to the difference between the 38 and the 200 kHz echograms $(S_{v_{200}} - S_{v_{38}})$ to separate fish with and without a swim bladder, following findings from several studies that fish with a swim bladder such as herring and capelin exhibit a stronger signal at 38 kHz while fish without a swim bladder, in particular mackerel, exhibit a stronger signal at 200 kHz (Gorska et al. 2004; Fernandes 2009; Korneliussen 2018). A running mean (window: 3 samples by 3 pings, approximately equivalent to 0.55 m x 18.5 m), was applied to smooth the echograms prior to subtracting the frequencies. A 5 x 5 dilation filter was applied to retain all features of the aggregations, and a bitmap was applied to mask the original S_v data with the virtual echogram.

The volume backscattering strength resulting from the previous steps was converted to the linear domain and integrated over the water column to a value of area backscattering coefficient (s_a, m^2 m^{-2}) for each 500 m segment of the survey:

$$s_a = \int_{z_1}^{z_2} s_v \, dz \,, \tag{3}$$

where z_1 and z_2 correspond to the upper and lower vertical limits of the vertical analysis domain, respectively.

The acoustic dead zone, i.e., the portion of the spherical acoustic beam where scatterers cannot be detected near the seabed, was estimated for each individual ping following Ona and Mitson (1996):

$$h_{eq} = 2404 \cdot \frac{(d_i - td_n) \cdot \tan\left(\frac{\emptyset_n \cdot \pi}{180}\right)^4}{{\emptyset_n}^2} + \frac{c_j \tau}{4} + bs \tag{4}$$

where d is the depth of the seafloor (m) for each ping *i*; td and $\emptyset$ are the transducer's depth (m) and the transducer's 3 dB half-beam angle (°) at 38 kHz for survey *n,* respectively; c is the sound speed (m s^{-1}) on day *j;* and τ and bs are the pulse duration (s) and backstep (m), respectively. The volume backscattering strength within the acoustic dead zone was replaced by the mean volume backscattering strength (MVBS) one meter above the dead zone for each individual ping.

2.3 ACOUSTIC SCATTERING WITHIN THE COLD INTERMEDIATE LAYER

Studies suggest that capelin exhibit a strong preference for temperatures between -1 and 3 °C (Rose 2005; Olafsdottir and Rose 2012; Ingvaldsen and Gjøsæter 2013). In the GSL during summer, this corresponds to the CIL. While direct observations are limited, Chamberland et al. (2022) used an indirect approach to demonstrate that capelin are likely predominantly distributed within this layer. The assumption was therefore made that capelin are constrained in large part to the CIL in the GSL and, thus, all echoes outside of the temperature range spanning -1 to 3°C were excluded. A high resolution (2 km), 3D temperature grid developed as part of the Atlantic Zone Monitoring Program (AZMP) was used (Galbraith et al. 2026) to define the upper and lower depth limits of the CIL. This allowed to reduce the probability of including redfish, Atlantic herring and Atlantic cod backscatter in the biomass estimates, although it is unlikely that Atlantic herring and Atlantic cod are excluded entirely. This method (hereafter referred to method "CIL") constitutes an upper limit for capelin biomass in the surveyed area as it includes backscatter from all swim bladdered fish within the CIL. All classification methods described in the following sections are also restricted to the CIL.

2.4 MACHINE LEARNING CLASSIFICATION MODELS

Two machine learning algorithms were tested, the support vector machine (SVM) and the random forest (RF), to classify capelin acoustic targets. The SVM (Vapnik 1995; Burges 1998) works by finding the optimal hyperplane in a N-dimensional space that separates the observations from the different classes in the feature space, and maximizes the separation margin between the observations of each class. SVMs are effective in high dimensional space (many variables). They are computationally efficient as they use a subset of training points (called support vectors) in the decision function. The RF (Breiman 2001) is a modification of bagging, where a collection of classification trees grown on bootstrap samples of observations, cast a vote on the most popular class. The unpruned trees and ensemble averaging work to reduce bias (the difference between the true mean and the average of the estimate) and variance (the expected deviation around its mean) (Hastie et al. 2009). The SVM and RF models were implemented in the R software

environment using the e1071 (SVM) and party (RF) packages (Hothorn et al. 2006; Strobl et al. 2007, 2008).

Information available from the biological samples were used to select acoustic targets corresponding to capelin, Atlantic herring and Atlantic cod (classes) (Table 1). Redfish were not included as their preferred habitat does not correspond with the CIL (Senay et al. 2023). Moreover, redfish stomach contents from the bottom-trawl surveys indicate a low incidence of capelin predation (Senay et al. 2023), further suggesting little vertical overlap between capelin and redfish habitat. Only clear acoustic targets validated by the bottom trawl or the pelagic trawl were used in the development of the classification method. Selected aggregations were all validated with trawl samples that contained more than 80% of the target species relative to all other swim bladdered fish present, to ensure that the acoustic signal was largely dominated by that species.

Acoustic data were subsampled over 100 pings and 5 vertical meters (hereby observations), to improve computational speed. The following variables were used as inputs for the machine learning models: mean S_v at 38 kHz, maximum S_v at 38 kHz, the difference in mean S_v between all possible pairs of available frequencies, as well as observation depth and bottom depth (m), for a total of 10 possible variables (see Table 4 for an overview of the variables in each model).

In total, 6, 5 and 9 aggregations were selected for capelin, herring and cod, respectively (Table 2). This resulted in a total of 20 aggregations (2446 observations). Although the aggregations are independent, the observations within each of them are not. As a result, the training and validation datasets were sampled from the aggregations rather than the observations, to ensure that the validation dataset did not contain observations from an aggregation that was also part of the training dataset. A training dataset was created by randomly selecting (without replacement) 75% of the aggregations. The remaining 25% was used for model validation. Each resulting dataset had to contain at least one aggregation of each class to be considered acceptable for model training and testing. Observations from each class were oversampled to the size of the dominant class, and normalized.

For the RF model, the number of classification trees was set to 500 and the number of predictors per split (m) was set to 3 as it minimized the out-of-bag error. The out-of-bag error is a performance metric calculated from the samples that are left out during bootstrapping, i.e. the out-of-bag samples. For the SVM model, the linear and radial kernels were tested. The linear model is computationally less expensive and assumes more simple decision boundaries within the feature space, as the data are separated by a linear hyperplane. The radial kernel can capture more complex relationships in the data, but can be subject to overfitting. A cost function (C) equal to 1 was used initially to find the best SVM model. For the radial SVM model, an initial gamma value of 0.25 was used.

The hyperparameter C represents the penalty applied to the model when an observation is misclassified. A greater C applies a higher penalty, which may lead to fewer misclassifications but may lead to overfitting of the model. The radial SVM includes a parameter, gamma, that describes the degree of curvature of the radial function. A smaller gamma may constrain the model too much and prevent capturing the complexity of the data. A larger gamma, on the other hand, may lead to overfitting because the area of influence of the support vector will only include the support vector itself.

For each model configuration, all possible combinations of 2 to 10 variables were evaluated and, for each of these combinations, a 10-fold cross-validation was used. The accuracy (K) and F1-score were used to evaluate the best model. The accuracy is estimated as the number of correctly

classified observations divided by the total number of observations. The F1-score is a combination of recall and precision (which are dimensionless quantities) and represents both bias and precision. It is calculated for capelin as follows:

$$F1\ score = \frac{2 \cdot Precision \cdot Recall}{Precision + Recall}, \tag{5}$$

where precision is defined as the number of true positives divided by the sum of true and false positives (value range: 0 to 1), and recall is defined as the number of true positives divided by the sum of true positives and false negatives (value range: 0 to 1). Values of F1 score vary between 0 and 1.

2.5 BOTTOM TRAWL SPECIES COMPOSITION

An additional method was conducted by classifying the acoustic scattering data following the species composition in the trawl (hereafter named method "COMP"). The proportion of area backscattering coefficient corresponding to capelin in stratum p was estimated as follows:

$$s_{a_{c_{y,n,p}}} = \frac{w_{c_{y,n,p}} 10^{\frac{TS_{c_{y,n}}}{10}}}{\sum_k \left[w_{k_{y,n,p}} 10^{\frac{TS_{k_{y,n}}}{10}} \right]} s_{a_{y,n,p}} \tag{6}$$

where w is the proportion of capelin c or swim bladdered fish species k relative to total catch of swim bladdered fish in stratum p, survey n and year y, and TS is the target strength ($TS = 10log_{10}(\sigma_{bs})$, dB re 1 m^2). The species proportions were obtained from the standardized trawl data averaged over each stratum.

The target strength was derived from a TS to mean length relationship for each swim bladdered fish species found in the biological samples, and is available from the literature (Table 3). Mean length for each species was estimated for the entire area for each survey and year.

Because of the low catchability of capelin in the bottom trawl data, especially compared to cod, this method will generally lead to an underestimation of capelin biomass, although it may lead to an apparent overestimation when compared to the acoustic data when capelin are found on the seafloor (due to potential herding and to the acoustic dead zone).

2.6 EXCLUSION OF STRATA

In this classification approach, strata containing high abundances of Atlantic herring and cod during the 2016-2020 period were excluded to reduce the contribution of these species to the acoustic backscatter. Trawl-derived biomass was standardized to a 15 minute tow duration at 3 knots, summed across all tows within each stratum, and then averaged across years. A constant trawl mouth opening was assumed. Strata were excluded when the resulting mean total biomass of herring or cod exceeded 5 kg (Figures 2 and 3). This filtering resulted in the exclusion of 28 strata in the nGSL and 14 strata in the sGSL. Although this approach likely leads to an underestimation of capelin biomass, it may still provide reliable temporal trends if the retained strata are representative of the overall distribution. This approach is hereafter named method "STRAT".

2.7 BIOMASS ESTIMATION

The classified s_a were converted to capelin density ρ (ind. m^{-2}) following:

$$\rho_{y,n,p} = \frac{s_{a_{y,n,p}}}{10^{\frac{TS_{y,n}}{10}}} \quad (7)$$

where TS represents the theoretical target strength of capelin as a function of length (Rose 1998), given by:

$$TS = 20 \cdot log_{10}(\bar{L}) - 73.1 \quad (8)$$

The mean length $\bar{L}$ of capelin was obtained as the standardized mean length for each year y and survey n.

Total biomass by stratum p for each survey/year was calculated as follows:

$$B_{y,n,p} = \rho_{y,n,p} \cdot \bar{W}_{y,n} \cdot A_p \quad (9)$$

where $\bar{W}_{y,n}$ is the standardised mean weight of capelin estimated for each year y and survey n.

3. RESULTS

3.1 ML MODEL PERFORMANCE

Results for the best-performing models including and excluding the depth variables are presented in this section. Because most of the capelin aggregations used to train and validate the models originated from the eastern Newfoundland region, the inclusion of depth variables may reduce model accuracy in the GSL, given substantial differences in ecology, physical water properties, and bathymetry among the two regions.

The best performance was obtained with the linear SVM conducted with the three following variables: maximum $S_{v_{38kHz}}$, $S_{v_{200kHz}} - S_{v_{38kHz}}$ and bottom depth (Table 4). The resulting F1 score was 0.87 and the K value was 0.84 on the validation dataset. When excluding the depth variables, the radial SVM yielded the best performance with a F1 score of 0.73 and a K value of 0.74, while the best linear SVM resulted in a F1 score of 0.74 but a K value of 0.65 – suggesting that it performed better at classifying capelin than herring and cod. The RF model performed relatively well when including the depth variables, with its best performance leading to a F1 score of 0.85 and a K value of 0.80 with 3 variables, but performed more poorly without the depth variables (K = 0.68; F1 score = 0.60).

Figure 4 shows the performance of the radial SVM as a function of the number of variables used. Values presented are the mean of the cross-validation results. When including the depth variables, the accuracy was relatively stable and high for models including between 2 and 5 variables; it then decreased gradually with the addition of new variables. Similarly, the F1 score was stable and high when including the depth variables, with a drop at the addition of the tenth variable. When excluding the depth variables, the accuracy and F1 scores were low when including few variables. They increased gradually with the addition of new variables before stabilizing at five variables.

In all cases, accuracy and F1 score were much higher when calculated on the test set than the validation dataset, suggesting that the models consistently overfitted. For example, accuracy of the best model (excluding depth variables) was 0.74 for the validation dataset (SVM*ra* in Table 4), but was 0.96 for the test dataset (data not shown).

The hyperparameter values that resulted in the highest performance for the best model were evaluated (SVM*ra*). The best values for hyperparameter C and gamma were 1 and 0.4, respectively, leading to both an F1 score and K value of 0.74 – a negligible improvement from the original performance of 0.73 and 0.74 for F1 score and K, respectively.

3.2 CAPELIN ABUNDANCE

Figures 5, 6 and 7 show total capelin biomass per year derived from each classification method in the nGSL, the sGSL, and in both areas combined. Total biomass from the bottom trawl catch is also shown ("CATCH"). Figure 7 includes total catch biomass from 1990 to 2020, to provide a better perspective on interannual variability.

As expected, method "CIL" resulted in the highest total biomass, while method "COMP" was consistently the lowest. In 2017, bottom trawl catch was higher than all acoustic methods, in both the nGSL and the sGSL, suggesting higher abundances of capelin near the seafloor. In the sGSL, this greater biomass resulted from a greater number of tows containing capelin compared to other years, while in the nGSL it resulted from a greater biomass being caught in a small number of tows. During that year, a peak in biomass was observed with both the "SVM" and "COMP" methods in the sGSL, but not with the other methods ("CIL" and "STRAT"). For method "COMP", this was the result of assigning a larger proportion of the backscatter to capelin that year, compared to other years. However, this would not explain the higher biomass observed with method "SVM". "CIL" biomass was low in 2017, indicating that the overall biomass of swim bladdered fish within the CIL boundaries was reduced that year.

In the nGSL, methods "CIL" and "STRAT" produced similar trends ($R_{spearman}$ = 0.9), while methods "COMP" and "SVM" showed comparable results ($R_{spearman}$ = 0.7). Other methods were more variable: "STRAT" broadly followed "COMP" and "SVM", but to a lesser degree ($R_{spearman}$ = 0.6 and 0.5, respectively), "CIL" and "STRAT" showed elevated biomass in 2016, and "CATCH" indicated a biomass decline that year. In the sGSL, methods "CIL" and "STRAT" also showed similar trends ($R_{spearman}$ = 1.0), and both closely tracked method "COMP" ($R_{spearman}$ = 0.8). All three methods were also in good agreement with trawl-derived biomass estimates ($R_{spearman}$ = 0.9). Correlation between method "SVM" and other acoustic methods was poor in the sGSL ($R_{spearman}$ = 0.3).

Apart from 2017, trawl-derived biomass between 2016 and 2020 was low compared to historical values, although variation is high (Figure 7). Trawl-derived biomass in 2017 was in the average range of historical values.

3.3 CAPELIN DISTRIBUTION

Figures 8 to 12 show mean biomass (kg m^{-2}) by stratum for each classification method, as well as for the trawl catch. Capelin distribution in the GSL varied depending on the classification method used. Overall, a higher density was observed in the northern portion of the sGSL, between Gaspé and the Magdalen Islands, along the Lower North Shore, and in the Strait of Belle Isle. High densities were also observed in the Laurentian Channel between Gaspé and Anticosti Island.

Figure 12 shows a high density of capelin on the Lower North Shore with method “CATCH”, largely responsible for the high total biomass in 2017. Cod and herring were also present in this area; this region was indeed excluded from method “STRAT”.

Mean total biomass between 2016 and 2020 was almost three times higher in the nGSL than the sGSL with method “CIL”, and 2.5 times higher with method “CATCH”. The difference was less pronounced with methods “COMP”, “STRAT” and “SVM”, where the mean biomass was 1.1, 1.8 and 2.0 times higher in the nGSL than the sGSL, respectively.

Using method “CIL”, the density of the acoustic backscatter (Figure 13) corresponding to swim bladdered fish within the CIL boundaries was on average 6 times higher when the CIL touched the seafloor compared to when it did not (mean 2016-2020), suggesting that fish were more tightly aggregated when near the seafloor. The integrated acoustic backscatter s_a (Figure 14) was also higher on average, but to a lesser extent (1.7 time higher). Although not uniform as hypothesized by Chamberland et al. (2022), it was more evenly distributed. Here, s_a is the mean s_v multiplied by the CIL thickness. Results were similar when constrained to strata where low occurrences of Atlantic cod and herring were observed (method “STRAT”).

4. DISCUSSION

4.1 ML CLASSIFICATION

The best model performance was achieved with the linear SVM that included the bottom-depth variable (Table 4). In this study, species classes appeared well separated by bottom depth (Figure 15). Unfortunately, the bottom depths associated with the acoustic targets used for model training are not necessarily representative of the typical depths at which these species occur in the GSL, for several reasons.

First, four of the six capelin aggregations used in the analysis were located off eastern Newfoundland rather than in the GSL, and their preferred bottom depths may therefore differ from those in the study area. Second, the selection of validated targets was biased toward near-bottom aggregations, because GSL aggregations could only be validated through bottom-trawl samples. Consequently, it is highly likely that incorporating bottom depth into the model and applying it to the GSL would yield inaccurate classifications.

When the depth variables were excluded, the radial SVM produced the best performance, with F1 and K values of 0.74 on the validation dataset and of 0.98 and 0.96 on the training dataset, respectively. The large discrepancy between the training and validation results indicates that the model overfitted. This outcome was expected, given the very small number of aggregations (15) available for training. Increasing the number of aggregations in the training dataset would likely reduce the apparent performance of the training dataset, but could improve its performance on the validation dataset. All frequencies were important to the classification, as reflected in the 5 most important variables identified in the best performing model (Table 4).

Due to computational limitations, an averaging cell of 100 pings by 5 meters was used to conduct the classification. While this approach greatly improves processing efficiency, it also results in the loss of some important features. For instance, Atlantic cod often appear as individual targets in the echograms, but those cannot be resolved at the scale of the cell averaging. Moreover, with such large averaging cells, targets of different species may be averaged out into one cell.

Many acoustic classification models have been developed using schools rather than cells (Fernandes 2009; Proud et al. 2020; Rousseau et al. 2022). The reduced variance within schools often leads to improved classification performance (Korneliussen et al. 2016), and the explicit school boundaries allow school-level descriptors to be incorporated into the models. Unfortunately, school-based classification was not feasible with the dataset used in this study, due to the large variety of aggregation shapes and sizes. School detection algorithms are better suited for 1) day-time acoustic data, when fish tend to form compact, well-defined schools, and 2) surveys targeting a specific region with lower species diversity.

Capelin are often found as large, diffuse clouds in the water column, however they can also form tight schools. Fish behaviour differs greatly between day and night, but the opportunistic surveys took place on a 24-hour schedule. On a daytime-only dataset, conducting the classification on schools rather than cells may improve the results. Limiting the survey area to regions of known capelin dominance would likely reduce diversity in the dataset and improve performance.

The fact that most capelin aggregations were obtained from the eastern coast of Newfoundland may also contribute to lower accuracy of the model when applied to the GSL if, for example, length distributions or habitat differ between the two areas.

4.2 CATCHABILITY

The overall total biomass was low when compared to survey values of Boudreau et al. (2023) and to commercial catch data. Boudreau et al. (2023) applied catchability factors *q* of 0.10 and 0.01 to the catch data in strata where the CIL was found to be resting on the seafloor or located higher in the water column, respectively.

In this study, a catchability factor and a standard deviation of 0.24 ± 0.12 was obtained across the 4 years (excluding 2017) in strata where the CIL rests on the seafloor, and 0.13 ± 0.04 in strata where the CIL is higher in the water column, when comparing total catch and acoustic biomass estimates per year. These values were estimated from method “CIL”, which is considered to be an upper limit for capelin abundance in the survey area. Values were similar when limited to the nGSL; however, catchability was found to be lower, although not statistically so, in the sGSL (0.01 ± 0.25) when the CIL was located higher in the water column.

Catchability factors estimated for the nGSL and the sGSL, regardless of the CIL’s position relative to the seafloor, were 0.18 ± 0.12 and 0.25 ± 0.23 (N=4 years), respectively.

Including only strata where low abundances of Atlantic herring and cod were observed, compared to capelin (method “STRAT”), resulted in *q* values of 0.58 ± 0.32 and 0.22 ± 0.12 when the CIL rests on the seafloor and when it is located higher in the water column, respectively. These values are likely more realistic, as they would exclude species such as cod and herring, which are likely included within method “CIL”.

Note that year 2017 was excluded from catchability estimates, because the catch was abnormally high that year, leading to *q* values above 1.

O’Driscoll et al. (2002) reported a mean catchability *q* of 1.1 ± 0.3 when comparing acoustic scattering from capelin in the whole water column to an untargeted (multispecies) bottom-trawl survey, but a median *q* value of 0.08. They concluded that bottom-trawl surveys are unlikely to provide a reliable index of capelin abundance/biomass due to the imprecision of the catchability for capelin. In the present study, catchability factors were estimated from total biomass per survey

year rather than for each tow event, resulting in a reduced variance. When estimating catchability for each stratum, variability was higher, and median values tended to be lower that mean values, as found in O'Driscoll et al. (2002).

4.3 CAPELIN ABUNDANCE

All acoustic methods presented in this study showed similar inter-annual trends (R^2 = 0.9) for capelin abundance in the GSL. The year 2017 showed a higher abundance in the "CATCH" data compared to other years, while it showed a decrease with the "CIL" method. Year 2017 was characterised by increased freshwater runoff compared to previous years, and the CIL in August of that year was warmer than normal as described in Galbraith et al. (2018). The results indicate that capelin were found in larger numbers near the seafloor during the 2017 survey, increasing their availability to the trawl. Biomass was at a time series low during this survey year with methods "CIL" and "STRAT". This may indicate a decrease in biomass, but may also indicate that a larger portion of the fish were found either outside of the CIL depth range, or in the acoustic dead zone. Along the survey path, the CIL thickness in 2017 was similar to other years. Methods "SVM" and "COMP" showed an increase in biomass in the sGSL in 2017. This is not surprising for method "COMP", which is estimated following proportions of capelin in the trawl. Biomass estimated with methods "SVM" and "CIL" were equal that year, meaning that the SVM model retained all acoustic backscatter found within the CIL, unlike in other years. It could be hypothesized that a lower abundance of herring and/or cod allowed capelin to expand their habitat to areas usually restrained by the presence of predators or competitors, i.e. in regions of preferred temperature, and nearer to the seafloor. The total abundance estimates presented here (mean between 1 976 t and 32 716 t with the "COMP" and "CIL" methods, respectively) are low compared to commercial fishery landings, which amount to an average of 8 288 t between 2016 and 2020 in NAFO Division 4R alone (excluding 2017, where commercial catch was only 1 945 t, see Table 3 in Boudreau et al. 2023). It is possible that method "COMP" underestimates biomass, however, the "CIL" method represents an upper limit for biomass within the CIL boundaries.

In this study, biomass estimates were calculated using mean theoretical TS and weight per survey and year. It could be argued that a more precise estimate would be obtained from calculating these values for each stratum. However, this is complicated by the fact that a value of weight and length is required for each stratum, even when no capelin, herring and/or cod are present in the biological samples. It is to be noted that the influence of weight and length tend to cancel each other in equations 7 and 9. As a result, the impact of these parameters on the resulting biomass is reduced.

Whether the timing and coverage of the multispecies survey is suitable to provide a representative abundance index for capelin remains unclear. In this study, capelin biomass was often driven by isolated hot spots throughout the GSL. This was most pronounced with the trawl data, but was also observable with the acoustic data. The highest catches were found along the northern shore of the St. Lawrence Gulf and estuary, between Tadoussac and Pointe-des-Monts, and between Sept-Îles and La Romaine. These areas are also known for their high occurrence of humpback (*Megaptera novaeangliae*), fin (*Balaenoptera physalus*) and blue (*Balaenoptera musculus*) whales, which feed on krill and small pelagic fish, including capelin.

Capelin in the GSL spawn around June and July, although variation in timing is high. Spawning occurs west to east (DFO 1996), and the location and timing varies with water temperature (Rose 2005). Although preferred temperatures for adult capelin range mostly between -1 and 3 °C,

capelin are found in warmer waters during spawning (Rose 2005). These factors may influence capelin distribution during the August multispecies survey.

The hypothesis that capelin are mostly distributed in the CIL is an important assumption in this study. Although the temperatures found within the CIL correspond to capelin's preferred habitat outside of the spawning season (Rose 2005; Olafsdottir and Rose 2012; Ingvaldsen and Gjøsæter 2013), it is unclear to what degree other factors such as predation and feeding might impact capelin distribution.

Capelin habitat selection strategies are poorly understood, but it is likely that prey and temperature are two important factors that drive habitat selection (Mowbray 2002; Rose 2005; Ingvaldsen and Gjoester 2013). Studies suggest that presence of capelin near the seafloor might be affected by the presence of predators (e.g. cod) (Mowbray 2002; Fall et al. 2021). Adult capelin also occupy a narrow range of salinity, between 33 and 35 psu (Rose 2005). Capelin distribution may be associated with areas of high zooplankton accumulation, such as the head of canyons, shelves, and near slopes (McQuinn et al. 2015; Aarflot et al. 2020).

According to a study by Dalpadao and Mowbray (2013), *Calanus finmarchicus* was the main prey of smaller capelin (< 12 cm) on the eastern coast of Newfoundland and in the Barents Sea. Larger capelin (> 12 cm) preyed mainly on krill in the Barents Sea, while copepods remained the main prey off Newfoundland. In both regions, daytime feeding was more successful than night time feeding. Capelin exhibited diel vertical migration in the Barents Sea, but remained close to the seafloor off Newfoundland (Dalpadao and Mowbray 2013). This result is in agreement with an earlier study by Mowbray (2002), who observed no diel vertical migration by capelin on the eastern coast of Newfoundland. Jansen et al. (2025) suggest that only a small fraction of capelin follow prey to the surface to feed at night in Greenland waters.

It is uncertain whether capelin in the GSL perform diel vertical migration. In the present study, restraining the biomass estimates to daytime data led to lower biomass estimates in three out of five survey years in the nGSL, compared to the 24-hour time-series (Figure 16), using both methods "CIL" and "STRAT". This indicates that a higher abundance was found within the CIL at night time during those surveys. However, the opposite was found in the sGSL, where a higher total biomass was found in three out of five of the survey years when restraining the estimates to day-time data, indicating that in those surveys, lower abundances were found within the CIL at night.

5. CONCLUSION

This study evaluated the potential to develop an acoustic abundance index for capelin in the Gulf of St. Lawrence using opportunistic survey data. Acoustic approaches showed consistent interannual trends among acoustic methods and trawl catch data, suggesting they can provide useful information on capelin abundance variability. However, absolute biomass estimates differed between methods and were generally low when compared to commercial catches, reflecting important uncertainties.

The ML classification showed potential but was limited by small and biased training datasets, leading to overfitting and reduced applicability to Gulf conditions. More broadly, the opportunistic nature of the data constrained classification performance and prevented the use of more robust approaches such as school-based methods.

Catchability estimates were higher than values currently used for the bottom-trawl indices for capelin. In addition, while the CIL appears to influence distribution, capelin habitat use is likely driven by a combination of environmental conditions, predation, and feeding, which are not fully accounted for in current approaches.

Overall, acoustic data from multispecies surveys represent a promising step toward improved monitoring of capelin in the GSL. Further work is needed to increase validated datasets, refine classification methods, and better account for environmental drivers and habitat overlap to support the development of a reliable abundance index.

ACKNOWLEDGEMENTS

I would like to acknowledge the contributions made by the Canadian Coast Guard and the crew of the CCGS Teleost to DFO's multispecies bottom-trawl surveys in the Gulf of St. Lawrence, and to the Spring capelin survey on the eastern coast of Newfoundland. I would also like to thank Alexandre Théberge for his assistance with acoustic data processing, Peter Galbraith for providing the 3D temperature grid, and Fran Mowbray for providing the acoustic and trawl data associated with the 2019 capelin survey. Finally, I thank Hugues Benoît, Ron Lewis and Manuelle Beaudry-Sylvestre for reviewing the manuscript and for their thoughtful comments.

REFERENCES

Aarflot, J.M., Dalpadado, P. and Fiksen, O. 2020. Foraging success in planktivorous fish increases with topographic blockage of prey distributions. Mar. Ecol. Prog. Ser., 644: 129-142.

Boudreau, M., Chamberland, J.M., Girard, L., Boudreau, M., Benoît, H., Lehoux, C., Smith, A., Galbraith, P. and Plourde, S. 2023. Capelin in the estuary and Gulf of St. Lawrence (NAFO Divs. 4RST) in 2021. DFO Can. Sci. Advis. Sec. Res. Doc. 2023/018. v + 51 p.

Brautaset, O., Waldeland, A.U., Johnsen, E., Malde, K., Eikvil, L., Salberg, A-B. and Handegard, N.O. 2020. Acoustic classification in multifrequency echosounder data using deep convolutional neural networks. ICES J. Mar. Sci., 77(4): 1391-1400.

Breiman, L. 2001. Random forests. Mach. Learn., 45, 5–32.

Burges, C.J.C. 1998. A tutorial on Support Vector Machines for pattern recognition. Data min. Knowl. Discov., 2(2): 121-167.

Cabreira, A.G., Tripode, M. and Madirolas, A. 2009. Artificial neural networks for fish-species identification. ICES J. Mar. Sci., 66 : 1119-1129.

Chamberland, J.-M., Plourde, S. and Benoît, H. P. 2022. Biological characteristics, factors affecting catchability, and abundance indices of capelin in the southern and northern Gulf of St. Lawrence multi species bottom trawl surveys. DFO Can. Sci. Advis. Sec. Res. Doc. 2021/077. iv + 41 p.

Chamberland, J.-M., Bourdages, H., Desgagnés, M., Galbraith, P., Isabel, L., Ouellette-Plante, J., Roux, M.-J., Scallon-Chouinard, P.-M., and Senay, C. 2025. Preliminary Results from the 2024 August ecosystemic survey in the estuary and northern Gulf of St. Lawrence. DFO Can. Sci. Advis. Sec. Res. Doc. 2025/032. iv + 101 p.

Chashchin, A., Shlyakhov, V.A., Dubovik, V.E., and Negoda, S. 2015. Stock assessment of anchovy (*Engraulis encrasicolus* L) in northern Black Sea and Sea of Azov. *In* I. Zlateva, V. Raykov, & N. Nikolov (Eds.), Progressive Engineering Practices in Marine Resource Management, pp. 209-243.

Choi, C., Kampffmeyer, M., Handegard, N.O., Salberg, A-B., Brautaset, O., Eikvil, L. and Jenssen, R. 2021. Semi-supervised target classification in multi-frequency echosounder data. ICES J. Mar. Sci., 78(7): 2615-2627.

Dalpadado, P. and Mowbray, F. 2013. Comparative analysis of feeding ecology of capelin from two shelf ecosystems, off Newfoundland and in the Barents Sea. Prog. in Oceanogr., 114: 97-105.

Demer, D.A., Berger, L., Bernasconi, M., Bethke, E., Boswell, K., Chu, D., Domokos, R., Dunford, A., Fässler, S., Gauthier, S., Hufnagle, L.T., Jech, J.M., Bouffant, N., Lebourges-Dhaussy, A., Lurton, X., Macaulay, G.J., Perrot, Y., Ryan, T., Parker-Stetter, S., Stienessen, S., Weber, T. and Williamson, N. 2015. Calibration of acoustic instruments. ICES Cooperative Research Report, No. 326. 133 pp.

De Robertis, A., and Higginbottom, I. 2007. A post-processing technique for estimation of signal-to-noise ratio and removal of echosounder background noise. ICES J. Mar. Sci., 64: 1282-1291.

DFO. 1996. Capelin in the Gulf of St. Lawrence. Atlantic Fisheries, Stock Status Report 96/25.

DFO. 2024. Assessment of the Estuary and Gulf of St. Lawrence (Divisions 4RST) Capelin (*Mallotus Villosus*) stock in 2022 and 2023. DFO Can. Sci. Advis. Sec. Sci. Advis. Rep. 2024/021.

DFO. 2026. Stock assessment of Divisions 2J+3KL Capelin to 2025. DFO Can. Sci. Advis. Sec. Sci. Advis. Rep. 2026/025.

Echoview Software Pty Ltd (2023). Echoview® version 14.0. Echoview Software Pty Ltd, Hobart, Australia.

Fall, J., Johannesen, E., Englund, G., Johansen, G.O. and Fiksen, O. 2021. Predator-prey overlap in three dimensions: cod benefit from capelin coming near the seafloor. Ecography, 44: 802-815.

Fallon, N. G., Fielding, S. and Fernandes, P. G. 2016. Classification of Southern Ocean krill and icefish echoes using random forests. ICES J. Mar. Sci., 73(8): 1998–2008.

Fernandes, P. G. 2009. Classification trees for species identification of fish-school echotraces. ICES J. Mar. Sci., 66: 1073-1080.

Galbraith, P.S., Chassé, J., Caverhill, C., Nicot, P., Gilbert, D., Lefaivre, D. and Lafleur, C. 2018. Physical oceanographic conditions in the Gulf of St. Lawrence during 2017. DFO Can. Sci. Advis. Sec. Res. Doc. 2018/050. v + 79 p.

Galbraith, P.S., Chassé, J., Shaw, J.-L., Lefaivre, D., and Bourassa, M.-N. 2026. Physical oceanographic conditions in the Gulf of St. Lawrence during 2025. Can. Tech. Rep. Hydrogr. Ocean Sci. 418: v + 94 p.

Gjøsæter, H., Bogstad, B. and Tjelmeland, S. 2002. Assessment methodology for Barents Sea capelin, *Mallotus villosus* (Müller). ICES J. Mar. Sci., 59: 1086-1095.

Gorska, N., Ona, E., and Korneliussen, R. 2004. On acoustic multi-frequency species identification and separation of Atlantic mackerel, Norwegian spring spawn herring and Norway pout. ICES CM 2004/R: 18. 1-9.

Hastie, T., Tibshirani, R. and Friedman, J. 2009. The elements of statistical learning (London: Springer), 763 pp.

Hothorn, T., Buehlmann, P., Dudoit, S., Molinaro, A. and van der Laan, M. 2006. Survival ensembles. Biostatistics, 7(3): 355-373.

Hurlbut, T., and Clay, D. 1990. Protocols for research vessel cruises within the Gulf Region (demersal fish) (1970-1987). Can. Manuscr. Rep. Fish. Aquat. Sci. 2082: 143 p.

Ingvaldsen, R.B. and Gjosaeter, H. 2013. Responses in spatial distribution of Barents Sea capelin to changes in stock size, ocean temperature and ice cover. Mar. Biol. Res., 9(9): 867-877.

Jansen, T., Thorvaldsen, K.G. and Post, S. 2025. Diel vertical migration and feeding dynamics of capelin and cod in an epipelagic subarctic ecosystem in Greenland. Rev. Fish. Biol. Fisheries, 35: 1977-2002.

Korneliussen, R. J., Heggelund, Y., Macaulay, G. J., Patel, D., Johnsen, E. and Eliassen, I. K. 2016. Acoustic identification of marine species using a feature library. Methods Oceanogr., 17: 187-205.

Korneliussen, Rolf J. (Ed.). 2018. Acoustic target classification. ICES Cooperative Research Report No. 344. 104 pp.

MacLennan, D. N., Fernandes, P. G., Dalen, J., 2002. A consistent approach to definitions and symbols in fisheries acoustics. ICES J. Mar. Sci., 59(2): 365-369.

Marques, T.P., Côté, M., Rezvanifar, A., Albu, A., Ersahin, K., Mudge, T. and Gauthier, S. 2021. Instance segmentation-based identification of pelagic species in acoustic backscatter data. 2021 IEEE/CVF Conference on computer vision and pattern recognition workshops (CVPRW). IEEE, 4373–4382.

McQuinn, I.H., Plourde, S., St. Pierre, J.F. and Dion, M. 2015. Spatial and temporal variations in the abundance, distribution, and aggregation of krill (*Thysanoessa raschii* and *Meganyctiphanes norvegica*) in the lower estuary and Gulf of St. Lawrence. Prog. Oceanogr., 131: 159-176.

Mowbray, F. 2002. Changes in the vertical distribution of capelin (*Mallotus villosus*) off Newfoundland. ICES J. Mar. Sci., 59: 942-949.

Mowbray, F.K. 2014. Recent spring offshore acoustic survey results for capelin, *Mallotus villosus*, in NAFO Division 3L. DFO Can. Sci. Advis. Sec. Res. Doc. 2013/040. v + 25 p.

Murphy, H.M., Adamack, A.T., Lewis, R.S., and Bourne, C.M. 2025. Assessment of Capelin (*Mallotus villosus*) in NAFO Divisions 2J + 3KL to 2023. DFO Can. Sci. Advis. Sec. Res. Doc., 2025/022. iv + 39 p.

O'Driscoll, R.L., Rose, G.A. and Anderson, J.T. 2002. Counting Capelin: a comparison of acoustic density and trawl catchability. ICES J. Mar. Sci., 59(5): 1062–1071.

Olafsdottir, A.H. and Rose, G.A. (2012). Influence of temperature, bathymetry and fronts on spawning migration routes of Icelandic capelin (*Mallotus villosus*). Fish. Oceanogr., 21(2-3): 182-198.

Ona, E. and Mitson, R. B. 1996. Acoustic sampling and signal processing near the seabed: the deadzone revisited. ICES J. Mar. Sci., 53: 677-690.

Ona, E. 2003. An expanded target-strength relationship for herring. ICES J. Mar. Sci., 60: 493-499.

Proud, R., Mangeni-Sande, R., Kayanda, R. J., Cox, M. J., Nyamweya, C., Ongore, C., Natugonza, V., Everson, I., Elison, M., Hobbs, L., Kashindye, B.B., Mlaponi, E.W., Taabu-Munyaho, A., Mwainge, V.M., Kagoya, E., Pegado, A., Nduwayesu, E. and Brierley, E.S. 2020. Automated classification of schools of the Silver Cyprinid *Rastrineobola Argentea* in lake Victoria acoustic survey data using random forests. ICES J. Mar. Sci., 77(4): 1379–1390.

R Core Team. 2024. R: A language and environment for statistical computing. R Foundation for Statistical Computing, Vienna, Austria.

Rose, G.A. 1998. Acoustic target strength of capelin in Newfoundland waters. ICES J. Mar. Sci., 55: 918-923.

Rose, G.A. 2005. Capelin (*Mallotus villosus*) distribution and climate: a sea “canary” for marine ecosystem change. ICES J. Mar. Sci., 62: 1524-1530.

Rose, G.A. and Porter, D.R. 1996. Target-strength studies on Atlantic cod (*Gadus morhua*) in Newfoundland waters. ICES J. Mar. Sci., 53: 259-265.

Rousseau S., Gauthier S., Neville C., Johnson S.C. and Trudel M. (2022). Acoustic classification of juvenile Pacific salmon (*Oncorhynchus spp.*) and Pacific herring (*Clupea pallasii*) schools using random forests. Front. Mar. Sci., 9: 857645.

Rousseau, S. and Émond, K. 2024. Design and analytical methodology for the Atlantic herring (*Clupea harengus*) Summer acoustic survey in NAFO Divisions 4RSw (2019-2023). DFO Can. Sci. Advis. Sec. Res. Doc. 2024/061. iv + 30 p.

RStudio Team. 2024. RStudio: Integrated development environment for R. RStudio, PBC, Boston, MA.

Rubbens, P., Brodie, S., Cordier, T., Barcellos, D.D., Devos, P., Fernandes-Salvador, J.A., Fincham, J.I., Gomes, A., Handegard, N.O., Howell, K., Jamet, C., Kartveit, K.H., Moustahfid, H., Parcerisas, C., Politikos, D., Sauzède, R., Sokolova, M., Uusitalo, L., Van den Bulcke, L., Van Helmond, A.T.M., Watson, J.T., Welch, H., Beltran-Perez, O., Chaffron, S., Greenberg, D.S., Kühn, B., Kiko, R., Lo, M., Lopes, R.M., Möller, K.O., Michaels, W., Pala, A., Romagnan, J-B., Schuchert, P., Seydi, V., Villasante, S., Malde, K. and Irisson, J-O. 2023. Machine learning in marine ecology: an overview of techniques and applications. ICES J. Mar. Sci., 80: 1829-1853.

Ryan, T.E., Downie, R.A., Kloser, R.J., and Keith, G. 2015. Reducing bias due to noise and attenuation in open-ocean echo integration data. ICES J. Mar. Sci., 72: 2482-2493.

Savoie, L. 2014. Preliminary results from the September 2012 and 2013 bottom-trawl surveys of the southern Gulf of St. Lawrence and comparisons with previous 1971 to 2011 surveys. DFO Sci. Advis. Sec. Res. Doc. 2014/053. v + 127 p.

Senay, C., Rousseau, S., Brûlé, C., Chavarria, C., Isabel, L., Parent, G.J., Chabot, D., and Duplisea, D. 2023. Unit 1 Redfish (*Sebastes mentella* and *S. fasciatus*) stock status in 2021. DFO Can. Sci. Advis. Sec. Res. Doc. 2023/036. xi + 125.

Simmonds, J. and MacLennan, D. 2005. Fisheries acoustics: theory and practice. Blackwell Science, Second Edition. 437 p.

Strobl, C., Boulesteix, A. L., Zeileis, A. and Hothorn, T. 2007. Bias in random forest variable importance measures: Illustrations, sources and a solution. BMC Bioinf., 8(25): 1–25.

Strobl, C., Boulesteix, A. L., Kneib, T., Augustin, T. and Zeilis, A. 2008. Conditional variable importance for random forests. BMC Bioinf., 9(307): 1–11.

Vapnik, V.N., 1995. The nature of statistical learning theory. Springer, New York.

Yassir, A., Andaloussi, S.J., Ouchetto, O., Mamza, K., Serghini, M. 2023. Acoustic fish species identification using deep learning and machine learning algorithms: A systematic review. Fish. Res., 266: 106790.

TABLES

Table 1. Summary of the surveys used to train the capelin classification models. All surveys were conducted onboard the CCGS Teleost.

Survey ID	Dates	NAFO Divisions	Number of trawl stations	Number of aggregations
T1637	02 Aug – 01 Sep 2016	4RS	167	5
T661	01 Sep – 28 Sep 2016	4T	162	1
T1841	03 Aug – 01 Sep 2018	4RS	168	2
T896	07 Sep – 01 Oct 2018	4T	106	2
T901	06 Sep – 01 Oct 2019	4T	123	1
Tel199	01 May – 18 May 2019	3KL	34	4
T2012	12 Aug – 05 Sep 2020	4RS	147	2
T2137	25 Jul – 25 Aug 2021	4RS	149	3

Table 2. Summary of samples used in the classification model before balancing the dataset. Each observation represents a 100 ping by 5 meter averaged sample.

Classification	Number of observations	Number of aggregations
Capelin	1194	6
Herring	508	5
Cod	744	9

Table 3. TS to length relationships used in the calculation of capelin biomass and to separate acoustic scattering following species composition in the trawl (method "COMP").

Species	Equation	Reference
Atlantic herring	TS = 20 $\log_{10}$(L) – 67.3	Ona (2003)
Atlantic cod	TS = 20 $\log_{10}$(L) - 66.0	Rose and Porter (1996)
Capelin	TS = 20 $\log_{10}$(L) – 73.1	Rose (1998)

Table 4. Model best performance on the validation data set, with corresponding variables, using the initial hyperparameters described in section 2.4. In the model names, *r* stands for radial, *l* for linear, and *a* refers to models that only used acoustic variables.

Model	Variable 1	Variable 2	Variable 3	Variable 4	Variable 5	F1 score	K
SVM*r*	$mean\ S_{v_{38}}$	$maximum\ S_{v_{38}}$	$S_{v_{200-38}}$	$S_{v_{120-38}}$	$Bottom\ depth$	0.83	0.81
SVM*ra*	$mean\ S_{v_{38}}$	$maximum\ S_{v_{38}}$	$S_{v_{200-120}}$	$S_{v_{200-38}}$	$S_{v_{70-38}}$	0.73	0.74
SVM*l*	$maximum\ S_{v_{38}}$	$S_{v_{200-38}}$	$Bottom\ depth$	-	-	0.87	0.84
SVM*la*	$mean\ S_{v_{38kHz}}$	$maximum\ S_{v_{38}}$	$S_{v_{200-70}}$	$S_{v_{120-70}}$	-	0.65	0.74
RF	$S_{v_{200-38}}$	$Bottom\ depth$	-	-	-	0.87	0.81
RF*a*	$maximum\ S_{v_{38}}$	$S_{v_{200-120}}$	$S_{v_{200-70}}$	$S_{v_{200-38}}$	$S_{v_{70-38}}$	0.60	0.68

FIGURES

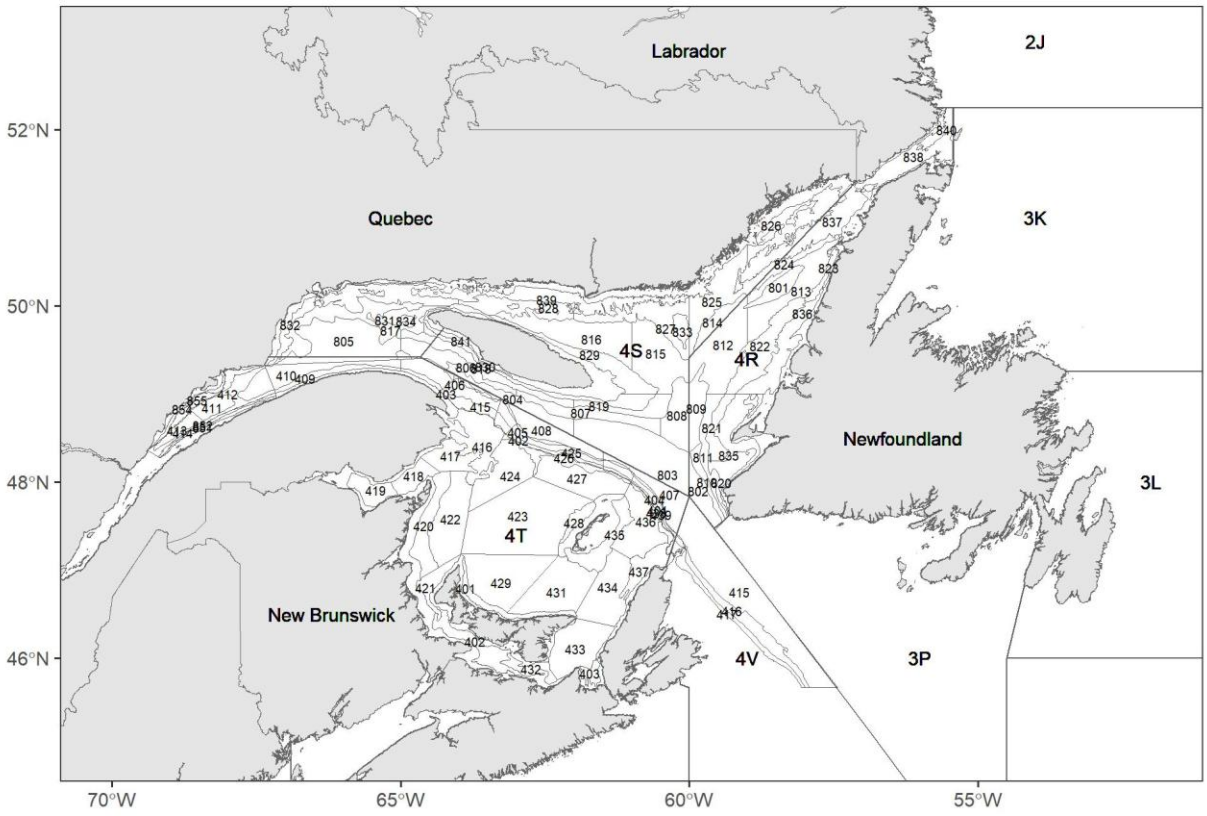


Figure 1. NAFO Divisions in the Gulf of St. Lawrence and the Newfoundland regions, and stratum definitions for the nGSL and sGSL annual bottom trawl surveys (grey polygons). Note that Divisions 3P and 2J are not included in this study.

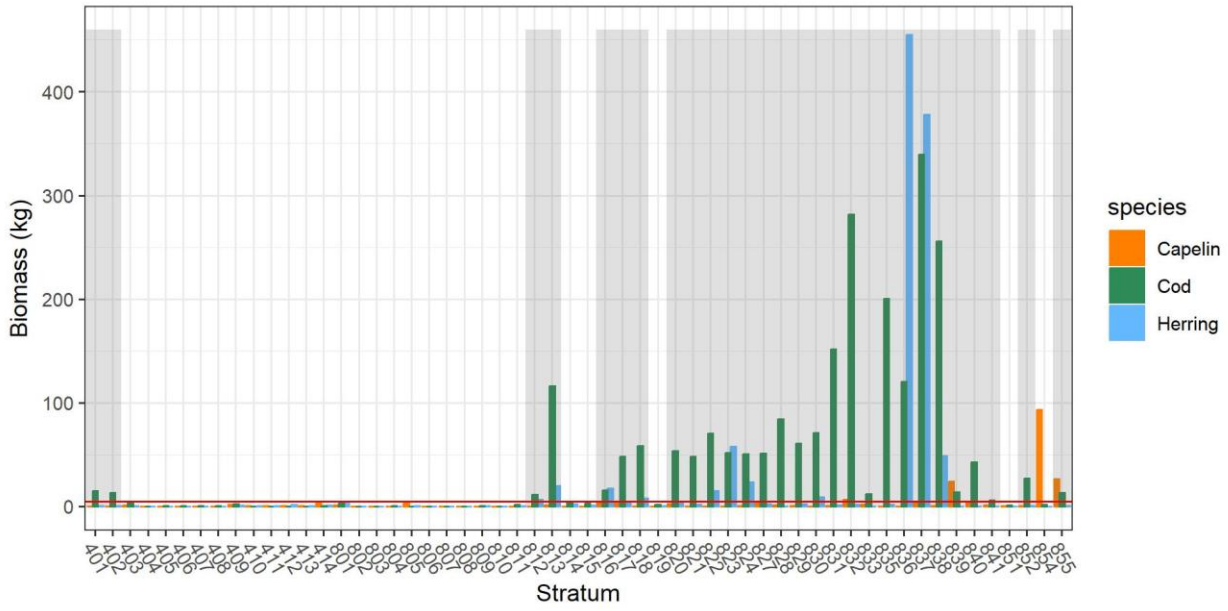


Figure 2. Standardized mean trawl biomass by stratum between 2016 and 2020 in the nGSL as obtained from the bottom trawl surveys. Shaded areas show strata excluded from method "STRAT". Red line represents the 5 kg cut off for exclusion of the stratum based on Atlantic herring and/or cod biomass.

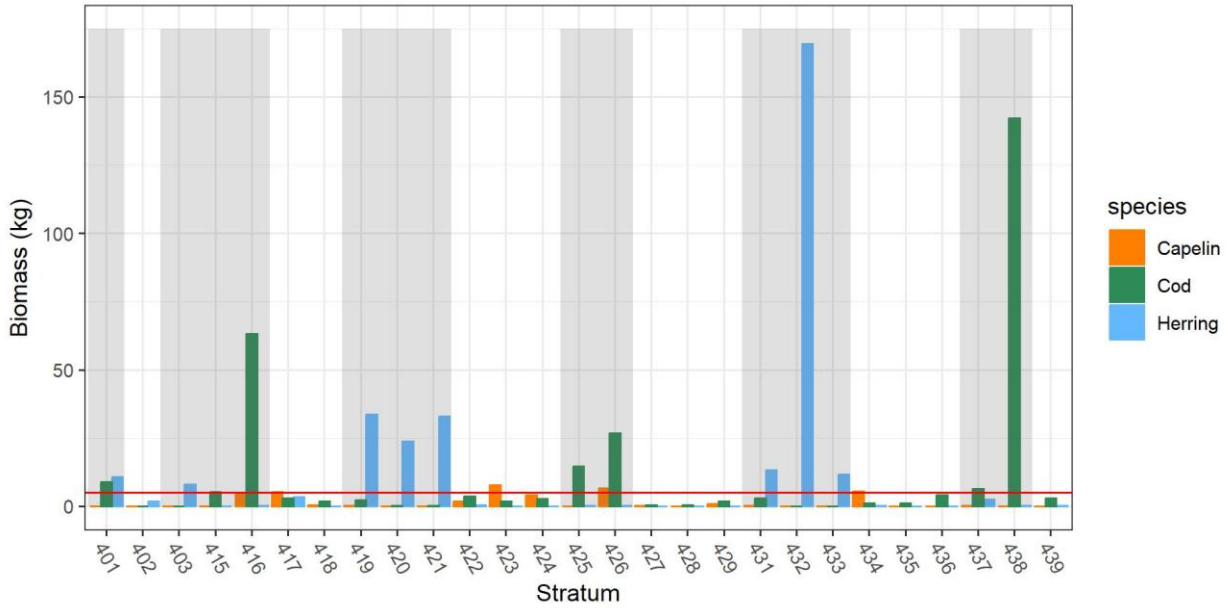


Figure 3. Standardized mean trawl biomass by stratum between 2016 and 2020 in the sGSL as obtained from the bottom trawl surveys. Shaded areas show strata excluded from method "STRAT". Red line represents the 5 kg cut off for exclusion of the stratum based on Atlantic herring and/or cod biomass.

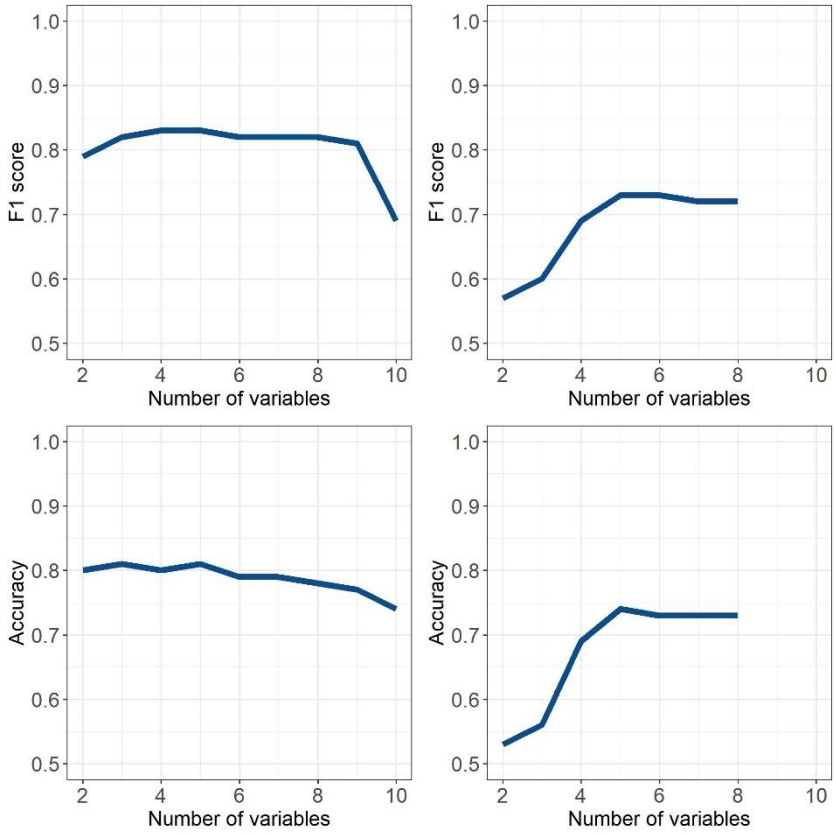


Figure 4. F1 score and Accuracy K as a function of the number of variables including (left panels) and excluding (right panels) the depth variables for the SVM with a radial kernel.

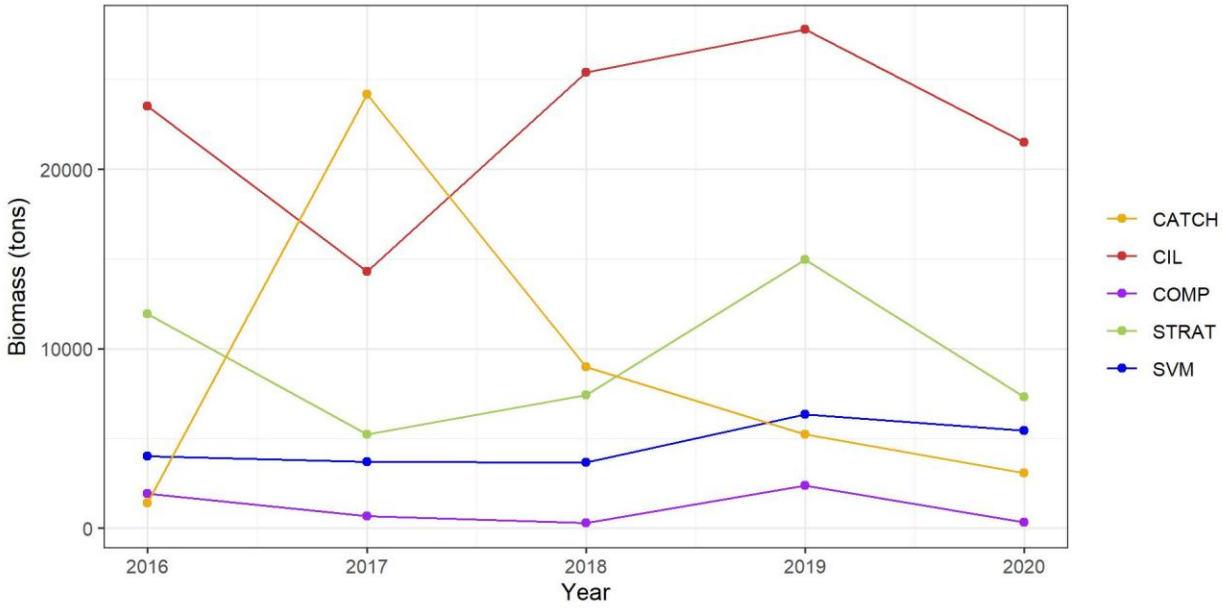


Figure 5. Total annual capelin biomass in the nGSL obtained with the classification methods presented in this study, as well as biomass derived from the bottom trawl survey ("CATCH").

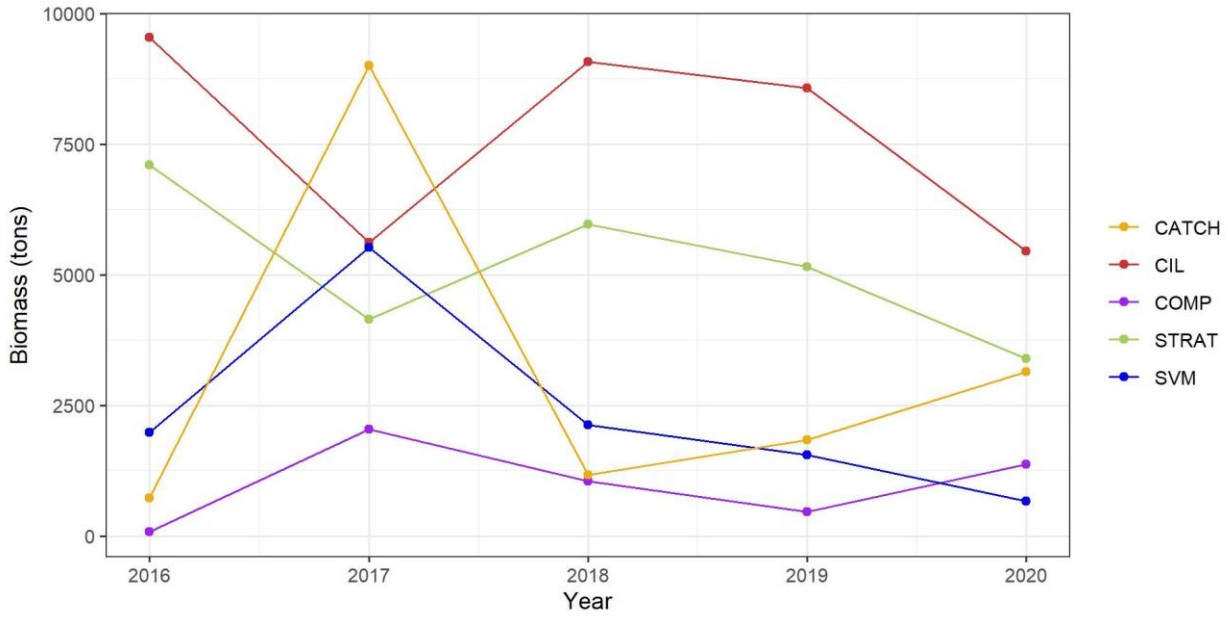


Figure 6. Total annual capelin biomass in the sGSL obtained with the classification methods presented in this study, as well as biomass derived from the bottom trawl survey ("CATCH").

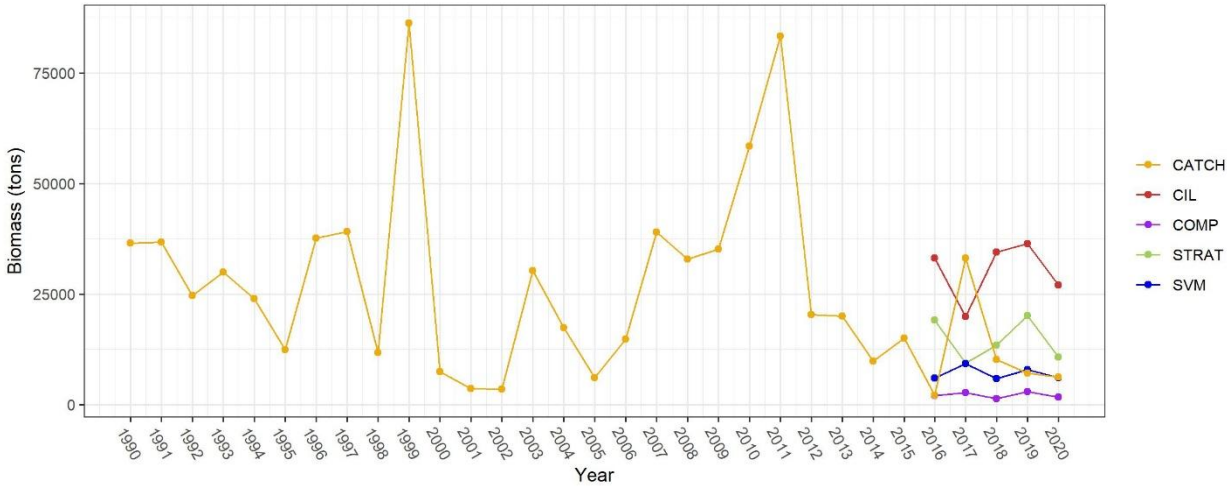


Figure 7. Total annual capelin biomass in the GSL obtained with the classification methods presented in this study, as well as biomass derived from the bottom trawl survey ("CATCH") from 1990 to 2020.

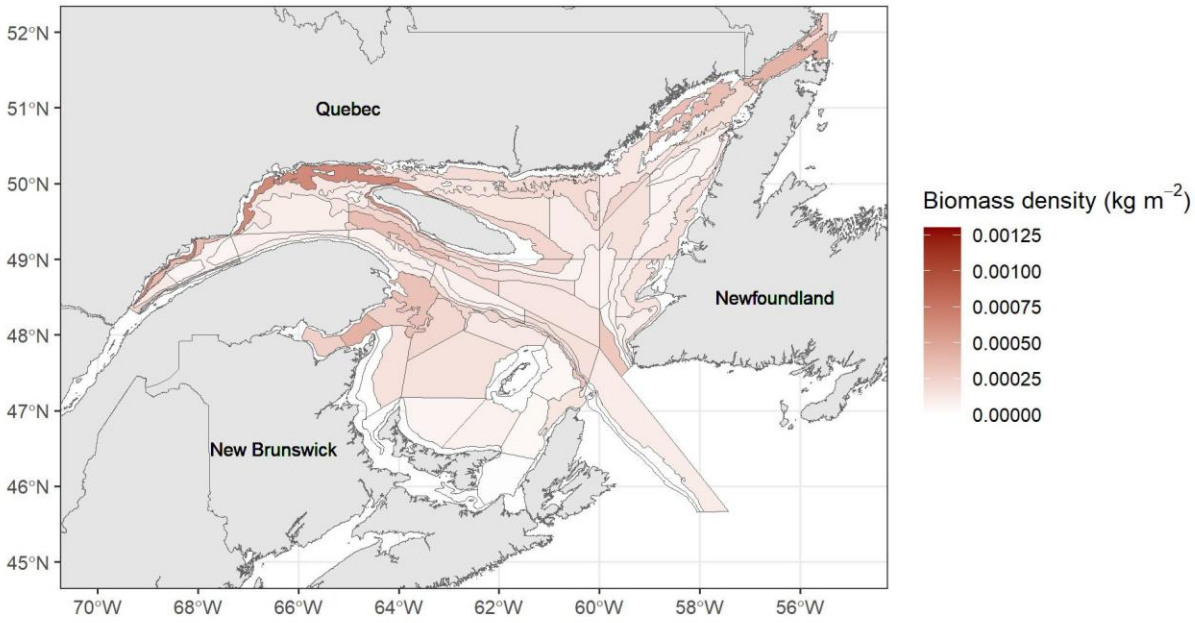


Figure 8. Mean biomass density (kg m^{-2}) estimated with method "CIL", all years of the acoustic study combined (2016-2020).

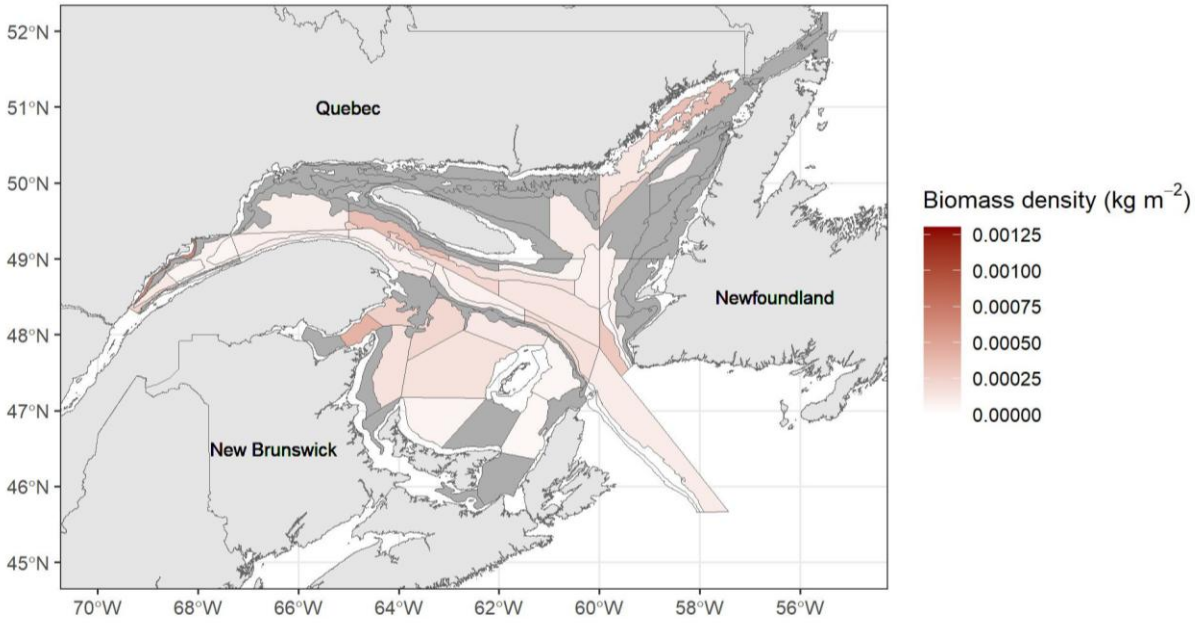


Figure 9. Mean biomass density (kg m^{-2}) estimated with method "STRAT", all years of the acoustic study combined (2016-2020). Excluded strata as shown in Figures 2 and 3 are shaded.

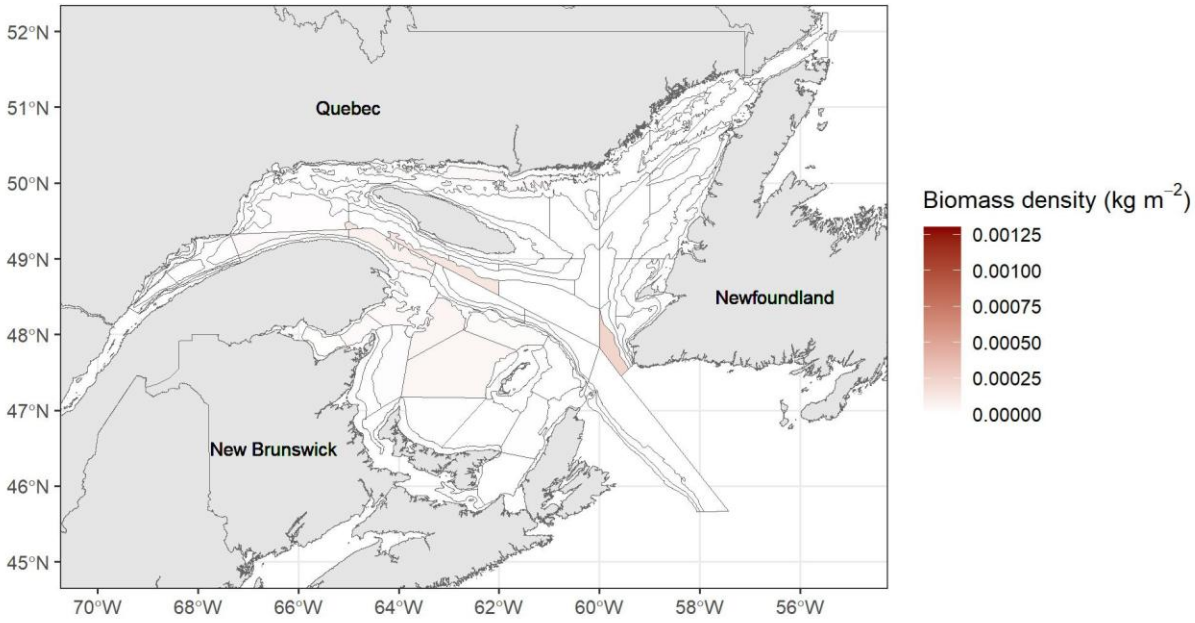


Figure 10. Mean biomass density (kg m^{-2}) estimated with method "COMP", all years of the acoustic study combined (2016-2020).

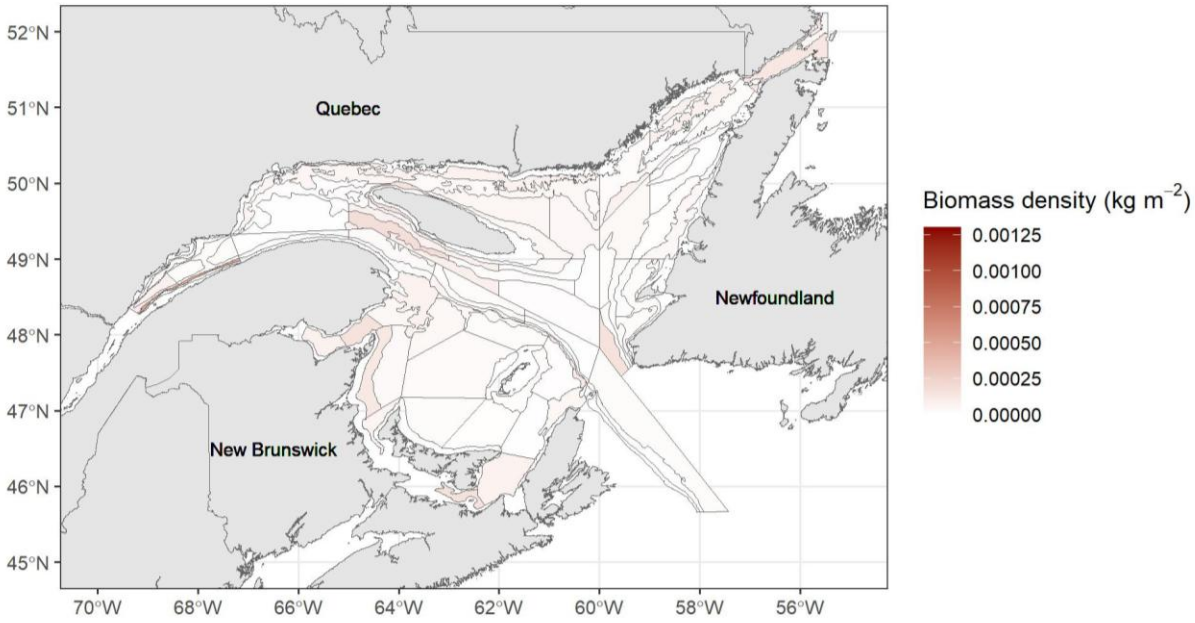


Figure 11. Mean biomass density (kg m^{-2}) estimated with the SVM, all years of the acoustic study combined (2016-2020).

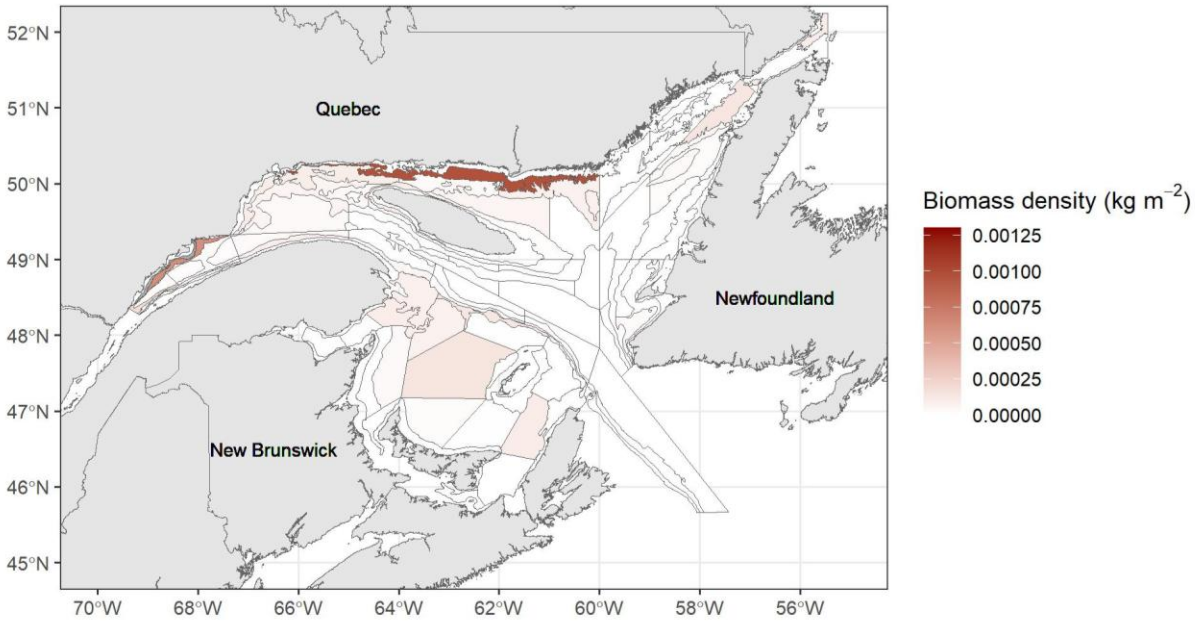


Figure 12. Mean biomass density (kg m^{-2}) from bottom trawl catch data ("CATCH"), all years of the acoustic study combined (2016-2020).

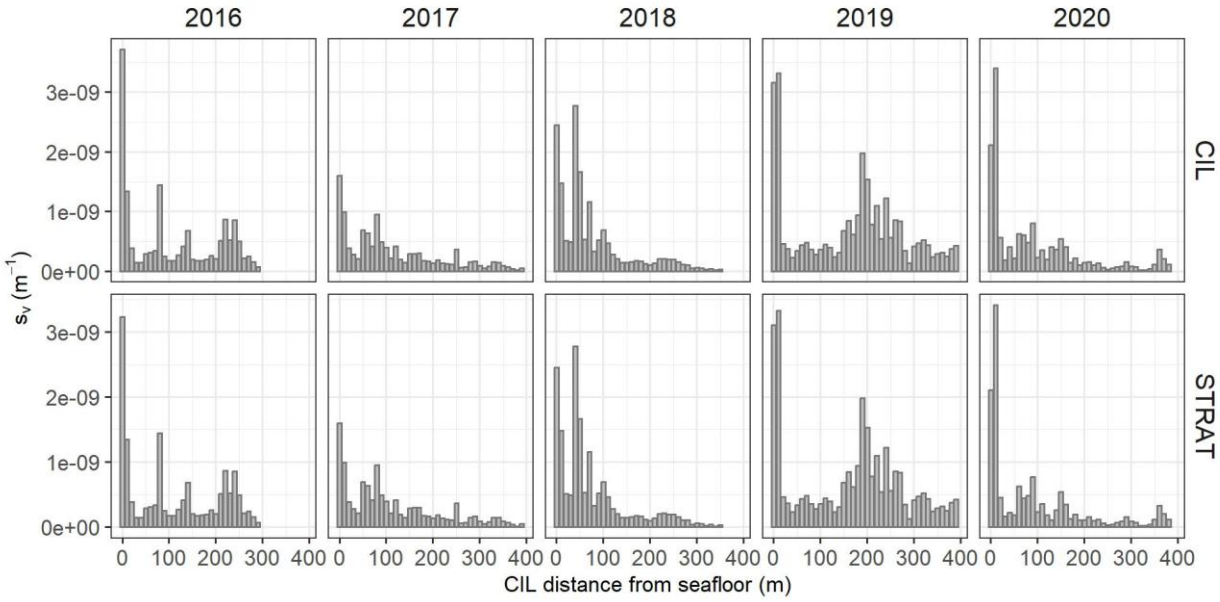


Figure 13. Mean volume backscattering coefficient (s_v m^{-1}) corresponding to swim bladdered fish within the CIL boundaries for each year of the acoustic study, using methods "CIL" and "STRAT", as a function of the distance separating the CIL from the seafloor, in the GSL.

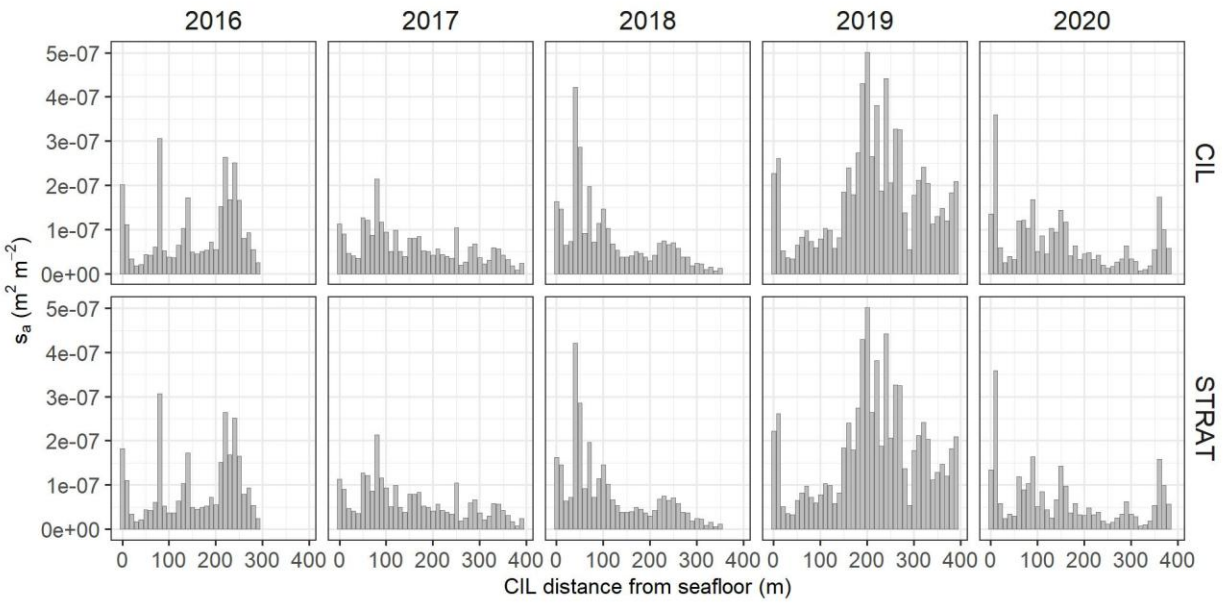


Figure 14. Mean area scattering coefficient (s_a, m^2 m^{-2}) corresponding to swim bladdered fish within the CIL boundaries for each year of the acoustic study, using methods "CIL" and "STRAT", as a function of the distance separating the CIL from the seafloor, in the GSL. s_a is equal to s_v multiplied by the CIL thickness.

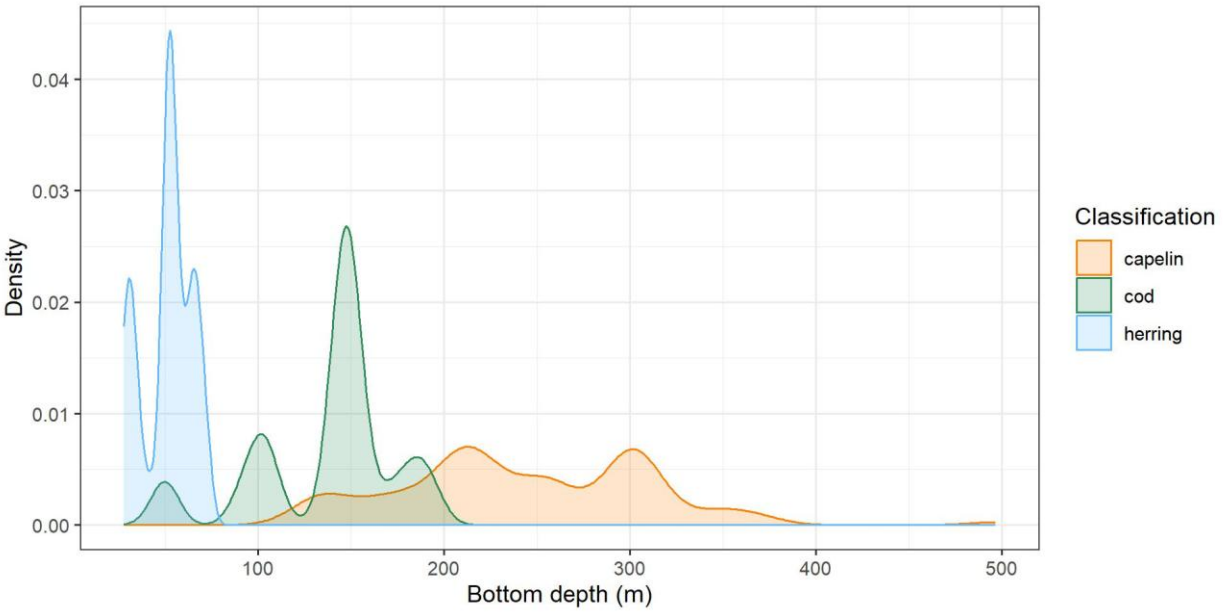


Figure 15. Bottom depth density functions corresponding to the 2446 observations used in the ML models.

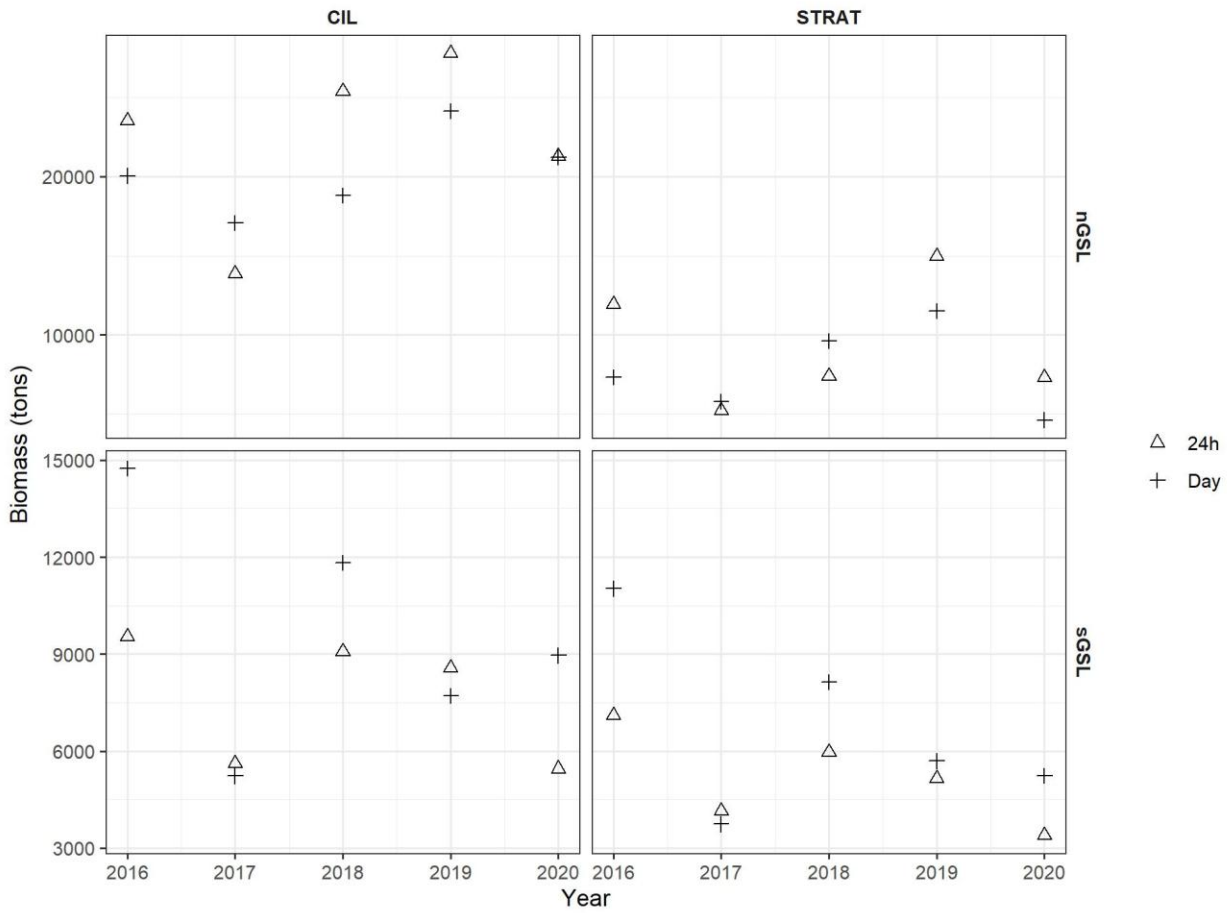


Figure 16. Total biomass in the nGSL and the sGSL including and excluding night time sampling, estimated with methods “CIL” and “STRAT”.